Studies on *C. elegans* probed with estradiol, elucidate the critical role of Na+/H+ exchanger, *nhx-2* in reproductive senescence and neuronal health

Shikha Shukla, Lalit Kumar, Arunabh Sarkar, Kottapalli Srividya and Aamir Nazir*

Division of Neuroscience and Ageing Biology, CSIR-Central Drug Research Institute, Lucknow-226031, INDIA

* Corresponding author:
Dr. Aamir Nazir (anazir@cdri.res.in)
Division of Neuroscience and Ageing Biology,
CSIR-Central Drug Research Institute, Lucknow-226031
Uttar Pradesh, India;
Telephone-+91-522-2772450 ext 4583

HIGHLIGHTS:

1. Silencing of a sodium proton antiporter *nhx-2* of gut ameliorates effects associated with alpha-Synuclein aggregation via mimicking dietary restriction in *C. elegans.*

2. We have established a genetic cross to construct a strain that expresses mCherry SIR-2.1 ubiquitously and α-Synuclein in muscles, that assists in corroborating the link between NHX-2 and SIR-2.1.

3. Human 17-β-Estradiol treatment induces the expression of *nhx-2*, through inducing the promoter specific histone H3 acetylation (H3K9) and lysine methylation (H3K4me3).

4. Effects associated with *nhx-2,* including prolonged reproductive span and neuroprotective effects, are SIR-2.1 driven.

5. *nhx-2* silencing decreases alpha-Synuclein aggregation however estradiol mediated overexpression above the endogenus level, does not amend the aggregation any further.

Abstract:

Setting in of reproductive senescence (RS) gives rise to several changes, making aged individuals susceptible to neurodegenerative diseases, cardiovascular and bone disorders amongst others. The present study deciphers the association of reproductive senescence, presence/absence of the sex hormone estradiol with age-associated neurodegenerative diseases. We employed RNAi induced silencing of a subset of 22 genes that are known to delay RS, followed by studies on alpha-Synuclein aggregation and associated effects in the transgenic *C. elegans*. These studies led us to fuctional characterisation of the Na+/H+ exchanger, expressed exclusively in gut. We found that RNAi of *nhx-2* ameliorates the affects associated with alpha-Synuclein aggregation via mimicking dietary restriction as it alters food absorption from the gut. Our studies further elucidated that such effects are Sir-2.1 driven as *nhx-2* RNAi did not delay reproductive senescence when *sir-2.1* was silenced concurrently. As estradiol plays a central role in both reproductive health as well as neuronal health, we performed structural binding analysis that demonstrated the binding potential of the estradiol receptor NHR-14 with *nhx-2* gene. Hence, we treated the worms with estradiol and observed that the transcription levels of *nhx-2* were elevated above the endogenous level. To unravel the underlying molecular mechanism of induction we performed ChIP analysis and it revealed that estradiol treatment gives rise to enhanced NHX-2 levels through inducing the promoter specific histone H3 acetylation (H3K9) and lysine methylation (H3K4me3).

Graphical abstract

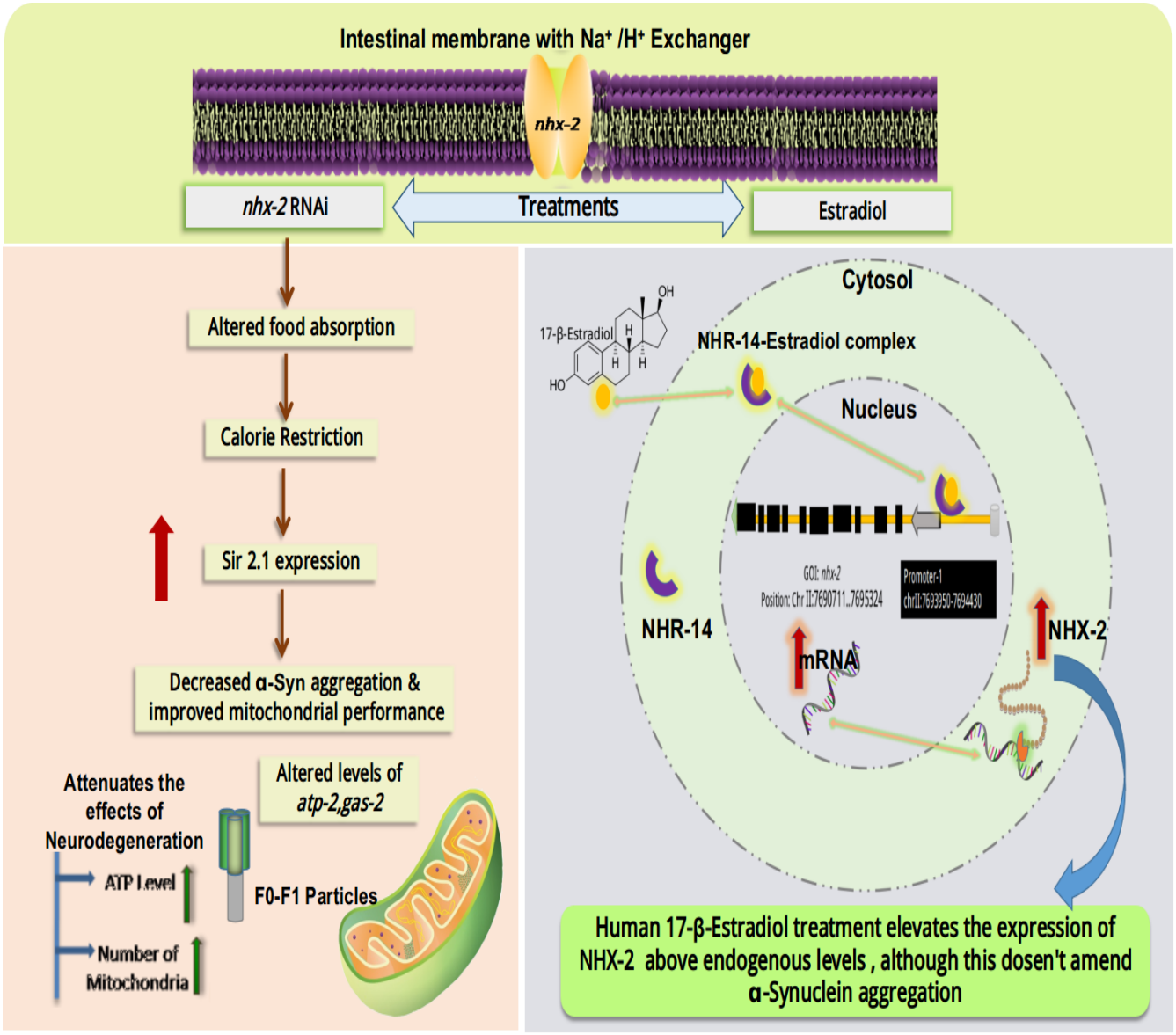

KEYWORDS:

nhx-2, Reproductive senescence, Calorie Restriction, Parkinson's disease, *C. elegans*, Sodium/Proton Exchanger, Estradiol

1.1 Introduction

Neurodegenerative diseases are multifactorial ailments involving various pathological mechanisms. The most relevant and known risk factors for neurodegenerative diseases include age, familial occurence, traumatic brain injury and cardiovascular diseases (1). There are other potential factors that add on to the susceptibility of the disease include inflammation, oxidative stress, hypertension, gender and endocrine imbalance amongst others (2). The major challenge in treating NDs is their multifactorial nature and lack of complete understanding of the cause and etiology (3). This may be the reason why most age-associated NDs have no cure yet. Hence it has become imperative to delve deeper into the understanding of multiple processes associated with ageing which may aid in devising complete cure for these ailments. One of the hallmark feature of aging is “reproductive senescence” (RS) - a gradual process that starts from the age of 35 and reaches its culmination at around 51 years of age (4). RS is characterized by several changes including a critical changes, which is decline in sex steroid hormones which are potent regulators of neuron survival (5-8). RS is not only followed by vasomotor symptoms like hot flushes, irritability, insomnia and mood disability but it may also make a person more vulnerable to several serious health conditions (9). It also puts one at a higher risk of osteoporosis, heart diseases, diabetes, hypertension, and breast cancer (10) thus making its association with NDs further intriguing. A study has also shown a low to moderate level of anxiety, depression, social dysfunction, and somatic symptoms and psychosocial stress in women going through reproductive senescence (11). Biochemical and neurophysiological studies report that fluctuations in these hormones, followed by reproductive senescence may affect cognition. It may also affect the cholinergic and serotonergic activity in specific regions of the brain (12), maintenance of neural circuitry, favourable lipoprotein alterations, and prevention of cerebral ischemia (13). Experimental, epidemiological and clinical evidence suggests, that sex steroid hormones have neuroprotective actions. Levels of estrogen and progesterone play a very critical role in the development of neurodegenerative disease (14). This perspective of pathology advocates that a variety of neurodegenerative diseases can be caused by reproductive senescence which causes a decline in sex steroid level and provides a novel therapeutic approach that may affect a broad spectrum of neurodegenerative diseases. Based on these facts, we hypothesize that molecular changes associated with reproductive senescence and gene expression modulations

induced by altered hormonal levels, may be associated with neurodegenerative diseases and warrant further deciphering of mechanistic aspects.

In the present study, we have carried out an in-depth analysis on RS related genes and their association with neurodegeneration having an aim of deciphering the link between healthy aging/longevity induced via prolonged reproductive healthspan and its impact on neuronal health. We studied genes that showed an affinity with the estradiol receptor and whose expressions are modulated upon the treatment of estradiol as this hormone is known to play a central role in reproductive senescence and neuroprotection. The course of our studies intricated the understanding of the interplay of reproductive span, gut homeostasis, calorie restriction and neuroprotection via sirtuins. A foundational study in 1935 in white rats reported that a dietary restriction extends lifespan between 30-50%, delaying death from age-related disorders and disease (15). The role of SIR-2.1 in calorie restriction is well established (16), and has been shown to be involved in neuroprotection in one of our previous findings (17). Our study herein, interestingly linked RS, ND and gut health under an umbrella and elucidated that Sir-2.1 is the central ground of the underlysing mechanisms involved in neuroprotective .

Our study, elucidates the association between RS, gut health, estradiol induced modulation of genes and their association with neurodegenerative disease.

1.2 Materials and methods

Strains used

Bristol strain N2 (wild type)

NL5901(Punc-54::α-Synuclein:: YFP + unc-119)

VC199(ok434) *sir-2.1*

UL2992[*sir-2.1*::mCherry + rol-6(su1006)]

VC363(ok553)/mIn1 [mIs14 dpy-10(e128)] II

AN105 [sir-2.1::mCherry + rol-6(su1006::Punc-54::α-Synuclein:: YFP + unc-119]

1.2.1 *C. elegans* strains and maintenance

Bristol strain N2 and NL5901 strain expressing "human" α-Synuclein protein in the muscles with YFP expression, VC199, UL2992 expressing *sir-2.1* ubiquitously, VC363 (obtained from the Caenorhabditis Genetic Centrer, University of Minnesota, St. Paul, MN, USA) were used in this study. *C. elegans* strains were cultured using standard protocols as described previously (18). *Escherichia coli (E.coli)* strain OP50 was used as standard food to feed the worms. Synchronized worms were obtained by embryo isolation procedure as described (19). Briefly, worms were washed with M9 buffer and treated with axenizing solution (2 ml of sodium hypochlorite and 5 ml of 1 M sodium hydroxide solution) until eggs were released from the body.

1.2.2 RNAi-induced gene silencing

Gene silencing was carried out as described previously employing the feeding protocol for the silencing of genes of interest (20). The dsRNA targeted for *C. elegans* gene expressed in bacterial clone (source Ahringer library) was cultured for 6–8 h in LB containing ampicillin (50 μg/ml). This bacterial culture was seeded onto NGM plates having 5 mM IPTG and 25 mg/L carbenicillin and incubated at 37 °C for 6-8 hours. Age-synchronous embryos of worms were transferred onto these plates for further experiments.

1.2.3 Imaging of α-Synuclein protein expression

To analyze the effect of *nhx-2* silencing on α-Synuclein aggregation, around 300 worms were grown on IPTG plates seeded with specific bacterial clones expressing dsRNA targeted at *nhx-2*. After 48 hours, worms were washed with M9 buffer to remove bacteria and immobilized with 100mM sodium azide (Sigma, Cat No. 71289). The imaging of live immobilized worms was carried out using a fluorescence microscope (Carl Zeiss Axio Imager M3). α-Synuclein expression was quantified through ImageJ software (ImageJ, National Institutes of Health, Bethesda, MD), and for fluorescence intensity measurement, ten worms were selected from every group to measure α-Synuclein expression.

1.2.4 ROS measurement

Quantification of ROS was performed in *C. elegans* by using 2,7-dichlorodihydrofluorescein diacetate (H_2DCFDA) (Invitrogen Cat. No. D399) as described previously (Jadiya & Nazir, 2012). Briefly, stock solution (10 mM) was prepared fresh in absolute alcohol, which was diluted (100 µM) in phosphate buffer saline (for 1 l PBS Na2HPO4 1.44 g, KH2PO4 240 mg, NaCl 8 g, and KCl 200 mg). Age-synchronized wild-type (N2) worms were raised either on bacteria with empty vector (EV) or bacteria-specific for RNAi of various genes of interest. After incubation for 48 h at 22 °C, worms were harvested using M9 buffer (for 1L KH_2PO_4 3 g, Na_2HPO_4 6 g, NaCl 5 g, and 1M $MgSO_4$ 1 ml) and suspended into PBS. Approximately 100 worms (following mean counting method) in 100 µl PBS were transferred into 96-well black plates (Perkin Elmer optiplate-96 F). H_2DCFDA at a concentration of 50 µM was added. Fluorescence intensity was quantified at 0 min after the addition of dye and 60 min after the addition of dye using Perkin Elmer multimode plate reader (Victor X3) at excitation 485 nm and emission of 520 nm. All the samples were estimated in triplicates, and for each group 300 worms were used.

1.2.5 Thrashing assay

Thrashing assay was performed with different treatment groups and the control group (EV). Worms were washed with M9 buffer and suspended on a glass slide in a drop of M9 buffer. Thrashes were counted as the bending of the head to the outermost angle of the body and then back to the previous posture of the body. Thrashing assay is considered to be a reliable behavioural assay to find out the levels of dopamine in the worms as thrashes are controlled by the dopamine concentration in *C. elegans*. Ten worms per group were counted for a mean number of thrashes per group and represented in a bar graph.

1.2.6 Food absorption assay

Food absorption assay was performed to check the amount of food absorbed in control as well as in RNAi conditions of *nhx-2*. After 48 hours, age synchronized worms were fed with fluorescent OP50 and were transferred on empty NGM plates for 1-2 hours to check the level of fluorescence that remained in the gut which signifies the bacteria that are still present in the gut and have not been absorbed by the worms; control group was studied as reference. Fluorescence was visualised with the help of confocal microscopy.

1.2.7 *in silico* studies

a) Prediction of the last PolyA signal and extracting invert repeats from the genes of interest, the respective gene sequences of *nhx-2* & *her-1* were obtained from Wormbase. PolyApred predicted the last PolyA signal of query gene sequences based on the score (21). RepEX server gave inverse repeats for the same query string and length was parameterized between 10-20 bases (22). The contigs that were located between the last polyA signal and exon of the query gene were taken as a template for further steps. b) Preparation of 3D-DNA, the contigs obtained from the prior step were given as a query to 3D-DART server for constructing the DNA with 3D coordinates (23). The parameters were kept as the default set of instructions by the server itself. The PDB files of the respective DNA-contigs were taken to the next step . c) Docking of β-estradiol with the NHR-14 receptor (UniProtKB - 002151). 3D structure of estradiol was downloaded from PubChem and NHR-14 structure from UniProt respectively (24) (25). Docking site prediction was done using PrankWeb (26). From this active sites were taken for the docking grid.. Docking was performed using AutoDock tool (27). From the docking results, the conformer with the least energy pose was taken as a hit for further steps. d) Docking of the NHR-14-estradiol complex with three different DNA contigs from two genes (*her-2* and *nhx-2*) to identify the potential binding affinity. Hex docking platform was used for the purpose where DNA contig was taken as a receptor and NHR-14 complex with estradiol was taken as a ligand (28). The resultant complex was then processed by CASTp for binding site analysis to visualize the binding pocket and interactive residues (29).

1.2.8 Quantitative Real-Time PCR (qPCR) studies for mRNA expression of various genes

The total RNA of the worms from control and experimental groups was extracted followed by the preparation of cDNA and quantification of mRNA levels of genes, employing qPCR. In brief, for RNA preparation, harvested worms were washed with DEPC (Sigma, Cat. No.D5758) treated water, and the RNA was isolated using RNAzol (Molecular Research Center, Cat. No.RN190) reagent. Isolated total RNA was then subjected to cDNA synthesis using Revert Aid Premium First Strand cDNA Synthesis Kit (Fermentas, Cat. No. K1652). The cDNA was used at a concentration of 125 ng and processed for quantitative real-time PCR using SYBR green master mix to quantitate the mRNA levels of genes, using actin as the loading control.

The amplification in 96-well plate was done with the program as (1) 1 cycle of Pre-incubation: 50°C for 2 minutes and 95°C for 10 minutes; (2) 40 cycles for Amplification: 95°C for 30 seconds, 55°C for 30 seconds, 72°C for 30 seconds; (3) Melting curve analysis: 95°C for 5 seconds, 65°C for 1 minute, (4) Cooling: 40°C for 5 minutes. After amplification, the Ct values were obtained which were used for the relative quantification of the mRNA expression of the target genes. The relative quantification was based on the $2^{-\Delta\Delta Ct}$ method.

Table: 1 – Sequences of primers used

Sn	gene	Forward Primer	Reverse Primer
1.	*nhr-14*	GTAGCACAAAGCGCAGAAAG	ACGGAGTTTCCCATCACTTC
2.	*nhx-2*	ATGCTTCTCTTCGGTTCAGTT	TCTCCGAACACGGCAATAAA
3.	*act-1*	TTACTCTTTCACCACCACCGCTGA	TCGTTTCCGACGGTGATGACTTGT
4.	*lin-45*	AGTCTGCCGAGATGTGCTTCTTCA	TTGTCACTTGTTCCTGCTCCTCCA
5.	*jkk-1*	GAAGCTGCTGCGTCGCATTTATCA	ACACAGCTTTACATTGCCGCTGTC
6.	*igg-1*	AACAACTTTGAGAAGCGTCGTGCC	ATCTTCTGGACGAAGTTGGATGCG
7.	*atg-5*	TGATGAAAGACGAGTCGGCACAGT	GTTTGGCAGTGATTAGGGCCTGTT
8.	*vps-34*	TGGATCCCTTTGCATCACGACGTA	CGAAACAATCCCAACACCACCGTT
9.	*atp-2*	TGTCTTGTCCCGTGGTATTG	GAGCAATGTCGTAGTGGTTCT
10.	*gas-1*	CGTGAGAAAGACCGAACCATAC	CTCCTCAATACGGCACAAGTATC

11.	*cco-2*	CGACTTTGCTTTGGCTGTTC	CAATGTAGGCGTAGACGGTATC
12.	*sir-2.1*	TCCAAGGCTGCTGAGCATTACTGA	TGATGAGCAAGACGAACCACACGA
13.	*rskn-1*	GAAGAGTTGTGTGAAGGAGGAG	AATGGACGTCTCCGTGTAATC
14.	*F36F2.2*	GATGTCGATGGTCCGAAGAAA	AATGGACGTCTCCGTGTAATC

1.2.9 Western blotting:

In order to validate the expression studies carried out by fluorescence microsopy of GFP expressing strains, western blotting was carried out using standard procedures. Worms were washed thrice with M9 buffer and re-suspended in phosphate buffer saline (PBS). These worms were sonicated in PBS containing protease inhibitor cocktail (Thermo Scientific 87785). Sonication was performed at 25 amplitude for 3 min (pulse time of 15 seconds); using a sonicator (Misonix S4000). The sonicated lysate was centrifuged at 6,000X g for 30 min at 4°C for removing debris, the supernatant contained total protein. Protein concentration was quantified using Bradford reagent (Sigma B6916). 40µg of total protein was loaded as calculated from Bradford assay and the same amount of soluble and aggregated proteins were loaded in 12 % sodium dodecyl sulfate-polyacrylamide gel electrophoresis (SDS-PAGE). Western blot analysis was performed as described previously using a standard protocol (30) . The primary antibodies used for western blot were monoclonal anti-α-Synuclein and monoclonal (1:1000, Abcam ab138501) and anti-actin antibody (1:1000, Santa Cruz sc-47778). Chemiluminescence detection was performed using LAS 3000 GE ImageQuent and densitometric analysis was performed by ImageJ software (Image J, National Institute of Health, Bethesda, MD).

1.2.10 Fecundity assay

To perform fecundity assay ten worms (age synchronized L4 worms) of each group N2, NL5901, and *nhx-2* knock out and *nhx-2* knock out in RNAi condition of *sir-2.1* were transferred on four different 90mm NGM plates and IPTG-NGM plates respectively. Worms were picked to fresh

plates every day and their eggs/offspring were recorded until there were no eggs remained on the plates in all the groups.

1.2.11 Genetic cross for creating transgenic strain that expresses mCherry Sir-2.1 and α-Synuclein:

To create a transgenic strain that expresses mCherry SIR-2.1 ubiquitously and α-Synuclein intact within its muscles, we performed genetic crosses between UL2992 and NL5901 followed by backcrossing with N2. For this standard procedures were followed, briefly, we first generated males of NL5901 strain by giving them mild temperature stress (30°c for 4-5 hours) and then placed the worm on normal 22°c which induced several male formations in next generation. To perform crossing we placed 8-10 worms of NL5901 and 3-4 hermaphrodites of UL2992 on 30 mm plates. We further chose those hermaphrodites from the progeny that showed α-Synuclein aggregation in muscles. To stabilize the strain we performed back cross with N2. This cross generated a strain that expressed mCherry *SIR-2.1* ubiquitously and α-Synuclein in muscles.

1.2.12 Measurement of mitochondrial content with the help of mitotracker

To check the effect of RNAi of *nhx-2* on mitochondrial content, worms were treated with mitotracker. To do so around, 300 worms were grown on IPTG plates having RNAi colony of strain HT115 to knock down *nhx-2*. After 48 hours, worms were washed with M9 buffer to remove bacteria and treated with Mitotracker (500 nM; Invitrogen cat. no M22426).

1.2.13 ATP measurement

Adenosine 5'-triphosphate (ATP) Bioluminescent Assay Kit (Sigma FLAA) has been used for ATP detection. Standard protocol with modifications utilized for ATP detection in *C. elegans*. Briefly, a fixed number of worms were collected from each group and proceeded for protein isolation as described above. The Bradford reagent is utilized for the measurement of the concentration of protein. After that 100µl ATP assay mix (2X10-12 stock) added into control and treatment vials and incubated for 3 min at room temperature. Further 50ug in 100 µl protein

sample was added into vials and for ATP measurement luminescence was measured through luminometer (Promega glowmax).

1.2.14 Cell isolation and MMP measurement

1.2.14.1 Cell isolation:

Method described by Zhang et al., (2011) has been followed for the cell isolation experiments. Age synchronized worms were pelleted via centrifugation at 13000 rpm for 2 min. Double distilled water was used for the washing of worm pellets.100 µl of the pellet was incubated for 4 min. in 200 µl of SDS-DTT solution (solution contains 0.25% SDS, 200 mM DTT, 20 mM HEPES, pH 8.0 and 3% sucrose) at room temperature. After treatment, 800 µl of egg buffer (containing 118mM NaCl, 48mM KCl, 2mM $CaCl_2$, 2mM $MgCl_2$, 25mM HEPES, pH 7.3) was added to the reaction. Worms were centrifuged at 13,000 rpm for 1 min in egg buffer and we repeated this step 5 times. For worm cuticle digestion, 15 mg/ml pronase (Sigma-Aldrich from *Streptomyces griseus*) enzyme has been used. Pronase added sample was incubated at room temperature for 20 min and during incubation for mechanical disruption we kept pipetting it. L-15 medium (Sigma-Aldrich L1518) was used for the termination of the digestion process and centrifuged at 180g for 5min on 4°C for sedimentation of cells. Cells were re-suspended in 1 ml L-15 medium and kept on ice for 15 min. 800 µl supernatant was separated into the fresh micro-centrifuge tube after ice settling step and centrifuged at 180g for 5min on 4°C

1.2.14.2 Mitochondrial membrane potential assay

For measurement of mitochondrial membrane potential worm cells were isolated as described above sub-section. Approximately, 1X10 5 cells/ml were suspended into serum-free media. Mitochondrial membrane binding dye JC-1 (2.5 µg/ml, Abcam ab113850) was used for staining for 15 min at 37°C. Cells were washed with serum-free media after incubation and potential was measured on a flow cytometer with excitation of 488nm and emission at 530 and 590nm.

1.2.15 ChIP Assay

Chip assay was performed essentially as described in this paper (31). Briefly, worms of transgenic strain NL5901 were grown till desired developmental stage (L4). After harvesting the

worms they were crossed linked with 2% formaldehyde. Worms were sonicated to yield DNA fragments in the range of 200–500 bp. sonication cycle was adjusted to 20 sec on, 59 sec off at 55 percentage amplification for 5 minutes and 15 cycles. After sonication the DNA was pooled down with the help of respective antibodies. ChIP assay was performed in both estradiol untreated and estradiol treated groups using the H3K9ac (Abcam, ab16635) and H3K4me3 (Abcam, ab8580) Antibodies and rabbit IgG as negative control. This was followed by qPCR analysis of promoter region of *nhx-2*. IDT was used to design the primers for promoter amplification. Following primers were used to amplify the promoter region

nhx-2 Promoter FP GCATGAGAGAGAGACGAGAGA

nhx-2 Promoter RP AGGAAATCTGACACGCAAGAC

These promoter regions were further amplified with the help of qPCR of *the nhx-2* gene. The sequence of the promoter was obtained from WormBase.

1.2.16 Statistical analysis

The graphical data were presented as mean ± standard error of the mean. The data between the two groups were statistically analysed employing Student's t-test by GraphPad Prism 5 software.

1.3 Results:

1.3.1 Preliminary screening of genes modulating reproductive health provides putative targets via modulating various endpoints associated with neurodegenerative disease (α-Synuclein expression, ROS, thrashing) in PD model of *C.elegans*

Several genes modulate reproductive health in *C.elegans*, for instance, RNAi of some of the genes delay reproductive senescence in *C.elegans* (32). Taking the studies with these genes forward, we investigated the effect of their silencing in reference to various endpoints of neurodegeneration. Firstly, we assayed α-Synuclein aggregation, by employing transgenic strain of *C.elegans* NL5901 [unc54p::α-Synuclein:: YFP + unc-119(+)] which expresses human α-Synuclein in muscles of the worm. We observed that RNAi of genes *T04B2.1*, *VC27A7L.1*, *F25H8.1*, *C34D10.2* and *rskn-1* increased α-Synuclein expression and RNAi of genes *daf-2*, *C25G4.10*, *F20B10.3*, *F36F2.1* and *nhx-2* decreased α-Synuclein expression. Control worms

exhibited a mean fluorescence intensity of 19.31 ± 0.5957 arbitrary units whereas *T04B2.1, VC27A7L.1, F25H8.1, C34D10.2* and *rskn-1* exhibited 22.03 ± 0.4810, 22.45 ± 0.5771, 24.45 ± 0.3211, 24.21 ± 0.8429, 22.23 ± 0.5497 and *daf-2, C25G4.10, F20B10.3, F36F2.1* and *nhx-2* exhibited a mean fluorescence intensity of 16.97 ± 0.4287, 16.85 ± 0.3447, 17.35 ± 0.4546, 16.11 ± 0.1126, and 17.50 ± 0.5640 arbitrary units respectively. (**Figure.1a-b).**

Age-associated neurodegenerative diseases are multifactorial. Among the many factors affecting neuronal ailments, reactive oxygen species (ROS) alteration plays a very crucial role (33). Hence, we studied the effect of RNAi of these genes on the level of ROS in the wild-type strain N2. We found that the level of ROS was 2.4,2.2,1.6,3.1,5.9,2.9,5.2,1.75,2.6, 2.3 and 1.7 folds down-regulated in *F25H8.1, moma-1, srz-1, C05D2.1, F20B10.3, ilys-3, F36F2.2, nhx-2, daf-2, sucg-1, C05E11.6* respectively and 1.2 fold up-regulated in both *VC27A7L.1* and *T04B2.1* (**Figure.1c)**.

Aberrant motility is a hallmark feature of PD and is directly associated with the concentration of dopamine present in *C. elegans* (34). To find out the effect of RNAi of these genes on the locomotion, we carried out a thrashing assay. Thrashing assay is useful for observation of the effect of loss of motor neurons. This assay was performed by counting the number of thrashes. We found that the number of thrashes was increased in RNAi groups of *sucl-2, daf-3, C24G4.10, VC27A7L.1, F20B10.3, F36F2.2, moma-1, nhx-2* and *CO5D2.3* significantly whereas in RNAi groups of *C34D10.2, T04B2.1, rskn-1* number of thrashes were decreased. (**Figure.1d)**

1.3.2 Western blot of anti-aggregated alpha-Synucleinn revealed that *nhx-2* RNAi not only decreases the YFP: alpha-Synuclein expression, it also decreases the aggregated form of alpha-Synuclein protein

To verify our finding we further performed an immunoblotting experiment using an anti aggregated alpha-Synuclein antibody and we found out that indeed *nhx-2* RNAi decreases aggregated alpha-Synuclein protein. The transgenic strain NL5901 fed with EV showed mean aggregation of 1.055 ± 0.05464 a.u. and worms fed with RNAi of *nhx-2* showed mean aggregation of 0.5072 ± 0.002500 a.u. which is significantly decreased. (**Figure.2a) (Figure.2b)**

1.3.3 Estradiol receptor shows affinity with the gene of *nhx-2* and Human 17-β- estradiol treatment alters mRNA levels of *nhx-2*

It is well known that estradiol plays a very crucial role in the reproductive cycle and health but other functions of estradiol have also been discovered. In the previous finding where reproductive senescence has been studied with respect to other health problems for instance osteoporosis, CVD and cancer (Shilbayeh, 2003); estradiol has been found to play a very critical role in all of them. Several studies show that estradiol plays a very significant role in the maintenance and survival of various neurons (35). The dimorphism of occurrence of Parkinson's disease in different genders and the timing of onset of reproductive senescence and neurodegeneration disease, presence of estradiol receptor in the brain in significant concentration and presence of estradiol receptor not only in nucleus but also in extranuclear sites including synapse (35) all of these provide a clue that estradiol could play a key role in connecting both reproductive senescence and ND. Hence we tried to check the effect of estradiol on the functioning of genes that is modulating various parameters of neurodegeneration.

a) *in silico* studies:

It is well known that hormone receptors are cytoplasmic receptors. In the presence of their respective ligands, they move inside the nucleus and bind with the hormone response element and control transcription of various genes. While they function in a ligand-responsive manner, their binding domains look after varied functions. The functionality of harmone response elements (HRE) is highly dependent on the position of receptor and the consequent recruitment of the co-participants in the regulatory complex through which transcription is affected (36). Translating the same insight to visualize the effect of *C. elegans* receptor of 17-β-estradiol NHR-14 and co integrator CBP-1 might affect the gene expression of *nhx-2*. To visualize if there is any binding affinity of the NHR-14 receptor with *nhx-2* gene's inverse repeats; we performed docking studies. The results (**Table-2**) showed that this binding could be site-specific as it was showing affinity towards inverse repeat (AGTTGCAATACTA) from position 1431-1443 in gene *nhx-2*, the active residues in the binding pocket were PHE , ARG , TRP, GLN, ASN, VAL, LEU, LYS and SER respectively whereas, NHR-14 didn't bind with another contig (GAAAAATTGTTCTA) from the position 1664-1667 of same gene . This obtained binding

domain interaction was cross-validated using *her-1* which is known to have interaction with NHR-14, obtained from gene ontology in BioGrid (37). The inverse repeat (TTTCATATCT) was taken from position 1578-1587 in gene. After docking the active residues participating in the binding pocket were ARG, SER, VAL, TRP, GLN, LEU, GLU, TYR, THR, PRO, GLY, and ILE. It was observed that the binding sites i.e interacting pockets were located at DNA binding domain of NHR-14 for positive docked contigs of both the genes i.e *nhx-2* and *her-1*. Hence it can be perceived from prior studies, literature and present docking that NHR-14 binds with the inverse repeats located upstream of the gene of interest which gives a clue that this gene could play a prominent and engaging role in Parkinson's disease and its pathophysiology.(**Figure.2e).**

Docking summary of NHR-14-DNA contigs from genes *her-1* and *nhx-2* respectively: Table: 2

S. No.	Gene	Inverse repeat Sequence (5'-3')	Position	Receptor	Interacting residues number in the active site	Active residues	Group
1	*nhx-2*	AGTTGCAA TACTA	1431-1443	NHR-14 estradiol complex	43,46,49,50,53,70,73,192,193,196,277, 278,279	PHE,ARG,TRP, GLN,ASN,VAL, LEU,LYS,SER	Hit Gene
2	*nhx-2*	GAAAAATT GTTCTA	1664-1667		No interaction	No interaction	Negative control
3	*her-1*	TTTCATATC T	1578-1587		46,47,48,49, 50,51,52,53, 54,55,73,96, 100,270,271, 272,274,275, 276,277,278,	ARG,SER, VAL,TRP, GLN,ASN, LEU, GLU,TYR, THR, PRO,GLY, ILE,	Positive Control

					281,282,283, 284,285,286, 288		

b)* Effect of human 17-β-estradiol on mRNA expression of *nhx-2

To check whether human 17-β-estradiol affects the mRNA levels of *nhx-2* or not, we treated transgenic worms with 17-β-estradiol and checked the level of *nhx-2* along with other screened genes. To do so, we treated worms with different concentration of estradiol 0.1 v/v, 0.3 v/v and 0.5 v/v, checked the level of estradiol-responsive vitellogenin gene and we found out that concentration 0.5 v/v increased the expression of both *vit-2* and *vit-6* gene, any further increase in concentration decreased *vit-2* expression **(Figure.2c)**. We found that upon 17-β estradiol treatment there were two genes whose mRNA levels were modulated namely *nhx-2* and *rskn-1*. So it validated our *in silico* data. The level of *nhx-2* was up-regulated whereas the level of *rskn-1* was down-regulated **(Figure.2d)**. Since RNAi of *nhx-2* was the one that modulated all the parameters of ND's and *rskn-1* did not show any such effects, we hypothesized that reduced level of *nhx-2* could play a crucial role in the maintenance of neuronal health. Hence it promted us to extent our further work to decipher the exact mechanical pathway involved in the associated effects.

1.3.4 ChIP analysis ascertains that estradiol treatment induces H3K4me3 and H3K9 acetylation activation of the promoter of endogenous *nhx-2 gene* thereby increasing its expression level

Once we deciphered that estradiol increases the transcription levels of *nhx-2*, we performed an *in silico* analysis and found that estradiol receptor NHR-14 shows significant affinity with the *nhx-2* gene. To assess that estradiol treatment leads to nhx2 induction by directly modifying the chromatin at its promoter, we analyzed the histone acetylation level at nhx2 promoter through chromatin immunoprecipitation (ChIP) assay, hence we investigated whether estradiol treatment is altering the epigenetic state of *nhx-2* promoter region. Prior to our study at the specific promoter, we first investigsated the effect of estradiol treatment on histone acetylation at the global genomic level, while the global expression of H3K9Ac was found to be significantly increased we found no significant alteration of H3K4me3 **(Figure.3b).** We further checked the occupancy of H3K4me3 and H3K9 acetylation activation marker of *nhx-2* promoter region after estradiol treatment with the help of ChIP analysis. The chromatin was first chipped with specific antibodies and then the chipped DNA was used to validate with the specific primers. Our results demostrated that human estradiol treatment gives rise to enhanced occupancy of both H3K4me3 and H3K3 acetylation markers on the promoter region of *nhx-2* thereafter resulting in increased expressions of the same. H3K9 acetylation marker was 2.167 fold and H3K9me3 marker was 3.8 fold upregulated on the promoter region of *nhx-2* upon estradiol treatment. Where untreated (UT) estradiol showed a mean fold change of 0.5374 ± 0.002896 and 1.586 ± 0.06830 , the estradiol treated worms showed a mean fold change values of 1.164 ± 0.04872 and 5.864 ± 0.07550 of H3K9 ac and H3K4me3 activations respetively. Hence our data stongly argues with our hypothesis that estradiol treatment increases the expression of sodium-proton pump in gut of C. elegans via inducing epigenetic modification on the promoter region of the *nhx-2* gene (**Figure. 3e).**

1.3.5 *nhx-2* upregulation does not increase alpha Synuclein aggregation any further

With the help of immunoblot experiment we checked the level of aggregated alpha Synuclein in both downregulated and upregulated (induced via estradiol treament) conditions of *nhx-2* and we found that although RNAi of *nhx-2* decreases the α-Synuclein aggregation significantly (where control NL5901 worms showed aggregation of 1.050 ± 0.05000 arbitrary units, RNAi of *nhx-2* showed aggregation of 0.5547 ± 0.05000 arbitrary units), increased expression of *nhx-2* via estradiol treatment, does not alter the aggregation any further. (**Figure.4a)**

1.3.6 RNAi of *nhx-2* decreases the absorption of food from the gut and mimics calorie restriction thereby exerting its effect on SIR-2.1 expression

In order to find out exact pathway of how RNAi of *nhx-2* affects various parameters of NDs, we mined the available literature on the subject, and we found that knockdown of *nhx-2* which is expressed in the apical membrane of epithelial cells, not only alters the intestinal pH, it is also associated with *opt-2* which is an oligopeptide transporter that helps in food absorption. (38). Hence we hypothesized that alteration in *nhx-2* expression might interfere with the food absorption and to ratify our hypothesis we carried out studies employing E. coli strain OP50 expressing green fluorescent protein (GFP). These fluorescent bacteria were fed to NL5901 and *nhx-2* knockout worms (VC363) towards assaying the level of food absorbed within them. We found that in *nhx-2* knock out condition significant amount of food remained in gut and rectum region in comparison to NL5901. Hence less food absorption exerts an effect like calorie restriction (CR), and probably this is how its RNAi is acting as a neuroprotectant. To test our hypothesis, we carried out further experiments .(**Figure.4b).**

After finding that *nhx-2* knockout /RNAi mimics CR and that it also exerts neuroprotective effect, we speculated that it might be affecting SIR-2.1 levels because based on previous findings it is known that CR exerts its neuroprotective effect in presence of SIR-2.1. Hence we checked the mRNA levels of *sir-2.1* in RNAi conditions of *nhx-2* and we found that in *nhx-2* silenced worms the levels of SIR-2.1 were more than fourfold upregulated (**Figure.4c).** We now know that *nhx-2* RNAi gives rise to increased mRNA levels of *sir-2.1* but we also checked whether this gets translated into increased protein levels of SIR-2.1 thereafter alters the function of SIR-2.1. In order to investigate this we conducted genetic crossing and fecundity assay.

1.3.7 RNAi of *nhx-2* extends reproductive life span only in presence of SIR-2.1 but it does not alter the brood size of transgenic strain NL5901:

To study the effect of *nhx-2* knockout upon reproductive life, the effect on the number of eggs laid per day and the number of eggs laid in the entire life span of transgenic strain NL5901 vs knockout strain of *nhx-2* VC363, we performed fecundity assay. We found out that wild type strain N2 starts laying eggs from day three and continues to do so until day ten, whereas transgenic strain NL5901 starts laying eggs from day three and continue to do so until day eight.

In case of an *nhx-2* knockout, worms start laying eggs from day three and keep on laying eggs until day thirteen. Whereas worms of *nhx-2* knockout strain VC363 showed no significant reproductive life extension in *sir-2.1* knockdown condition, they started laying eggs from day 3 and continued until day 9. Although there was no major difference between total numbers of eggs laid in entire lifespan in all the conditions as eggs laid per day was decreased as the days extended in case of *nhx-2* knockout worms. We found out that knockout of *nhx-2* increased the reproductive life span by 5 days altogether but this was governed via SIR-2.1 because in RNAi condition of SIR-2.1 there was no significant effect on the reproductive life span**.** .(**Figure.4d).**

1.3.8 Creation of a transgenic strain that expresses ubiquitous mCherry SIR-2.1 and α-Synuclein intact with its muscles signifies that *nhx-2* RNAi alters the expression of SIR-2.1

To substantiate our findings that knockdown of *nhx-2* exerts its neuroprotective effect via up-regulating the expression of SIR-2.1, we created a transgenic strain that expresses SIR-2.1 ubiquitously and α-Synuclein intact with its muscles. We performed several genetic crosses along with several backcrosses between transgenic strain UL2992 [sir-2.1::mCherry + rol-6(su1006)] that expresses mCherry tagged SIR-2.1 and transgenic strain NL5901 that expresses α-Synuclein intact with its muscles. With the help of genetic and backcross, we have constructed a strain that expresses mCherry tagged SIR-2.1 ubiquitously and YFP α-Synuclein in the muscles. We further performed *nhx-2* RNAi in this strain and we observed that knockdown of *nhx-2* in these worms, decreases α-Synuclein expression and increases SIR-2.1 expression. This experiment hence further substantiated our previous finding that *nhx-2* RNAi exerts its neuroprotective effect via modulating the expression of SIR-2.1.(**Figure.5).**

1.3.9 RNAi of *nhx-2* improves mitochondrial functioning and restores mitochondrial membrane potential in PD model of *C. elegans*

To find the exact pathway that was being affected via *nhx-2* RNAi first of all, we checked the levels of several genes of the various pathways for example; *lin-45, jkk-1, lgg-1, atg-5, vps-34, atp-2, gas-1*, and *cco-2* and we find out that mRNA levels of genes of mitochondria were being modulated. We found that *atp-2* which encodes the beta subunit of the soluble, catalytic F1 portion of ATP synthase (mitochondrial respiratory chain [MRC] complex V) was 17.36 fold up-regulated whereas *gas-1* whose expression is controlled by *atp-2* via feedback inhibition (39)

also down-regulated by 2.06 folds **(Figure.6a)**. The above sets a clue indicating that since knockdown of *nhx-2* is modulating a component of ATP synthase, it might be affecting the overall production of ATP and the number of mitochondria. To check their levels, we performed ATP assay and mitotracker imaging to know the content of healthy mitochondria in the knockdown condition of *nhx-2*. We found that the ATP level was 1.33 fold up-regulated **(Figure.6b)** and several mitochondria appeared to be increased significantly in *nhx-2* knockdown condition **(Figure.6c)**. Now the question was how does knockdown of a proton pump can modulate ATP levels and mitochondrial content ? To know the answer we checked the change in potential of the mitochondrial membrane which is responsible for proton gradient and thereby ATP production as well. To check the modulation in mitochondrial membrane potential of each cell we first of all isolated cells of *C. elegans* following the method described earlier. We checked out the change in mitochondrial potential in control wild-type worms, in PD model NL5901 and worms treated with knockdown of *nhx-2* in PD model NL5901 with the help of flow cytometry and we found out that RNAi of *nhx-2* is driving the membrane potential towards wild-type N2 strain by restoring mitochondrial depolarization **(Figure.6d) (Figure.6e)**

These experiments suggested that RNAi of *nhx-2* is exerting its neuroprotective effect by mimicking calorie restriction and improving mitochondrial membrane potential.

1.4 DISCUSSION

There has been a significant increase in human lifespan in last few decades. This increase in life expectancy of humans poses a great threat to age-associated health challenges including neurodegeneration. It has become imperative to explore trajectories that support healthy aging, in turn, protect from these ailments. Delaying reproductive senescence and increasing a healthy life span is an entirely new perspective in understanding the onset of ageing and age-associated diseases. When reproductive senescence sets in, it gives rise to several changes that affect the susceptibility of aged individuals towards several health conditions, for instance, cardiovascular diseases, osteoporosis, and neurodegenerative diseases. One major change that immensely concerns neuronal health is the change in blood levels of estradiol. The presence of estradiol receptor GPERs in brains cells, sexual dimorphism in the prevalence of different neurodegenerative diseases and other facts such as observational studies indicating estrogen use

in postmenopausal women and its association with reduced (25–70%) risk of neurodegeneration, prove that estradiol is an important factor in neuronal health and integrity (40).

In the present study, we have explored the role of such genes that are known to extend reproductive span in the context of neurodegeneration. In order to connect these genes with estradiol functioning, since estradiol plays a central role in connecting neuronal health with reproductive health, we studied human 17-β-estradiol induced effects on function, transcription and epigenetic modifications of the screened genes. With the help of data mining, *in silico* studies, functional genomics and molecular biology approaches, we have studied the role of 22 such genes that modulate RS with respect to various endpoints of neurological ailments such as α-Synuclein aggregation, ROS production, and dopamine levels through aversion assay. We further investigated whether human estradiol induces any modulation in the transcription levels of the screened genes to find out their relevance in neurodegenerative disease vis-à-vis healthy aging. These studies lead us to identification of *nhx-2*, a proton sodium anti-porter, which is expressed exclusively on the apical plasma membrane of the intestine. This finding corroborates that the gut homeostasis definitely plays a crucial part in neuronal health but estradiol regulate one of the genes of gut was a complete new finding. With the help of *in silico* analysis, we observed that NHR-14 which is the receptor of human estradiol in *C. elegans* shows affinity with the invert repeats present in the promoter region of the *nhx-2* gene. NHR-14 is a receptor that is present in the cytoplasm in the cell but when it binds with its ligand, it gets translocated into the nucleus and modulates the transcription of several genes. NHR-14 is a receptor of human estradiol and we found that it has the affinity to bind with the promoter region of the *nhx-2* gene. In order to ascertain our findings, we performed ChIP analysis to check the epigenetic modification on the promoter region of *nhx-2* gene. We checked the occupancy of H3K4me3 and H3K9 acetylation activation marker designing spercefic primers of the promoter region of *nhx-2* gene after estradiol treatment. We found that estradiol treatment gives rise to increased occupancy of both H3K4me3 and H3K9 acetylation marker in the promoter region of the *nhx-2* gene. Our this data strongly argues with our previous finding and signifies that estradiol governs the levels of this proton pump in gut. Now we know that estradiol gives rise to upregulation of *nhx-2* so it helped us to find out the other facet of the coin which is whether increased expression of *nhx-2* accelerates the alpha-Synuclein aggregation any further. However, we learnt that increased levels of *nhx-2* did not alter the alpha-Synuclein expression any further.

Our knowledge of the biological role of sodium-proton transporters in the intestine has been around pH maintenance, food absorption, lipid storage and larval development (38). In the present study, we observed the marked knockdown effect of the sodium-proton antiporter on neurodegenerative disease in *C.elegans*. Our observations substantiate previous findings that the loss of *nhx-2* gives rise to alteration of pH which leads to a phenotype that mimics starvation and we further found that the effect exerted via RNAi of *nhx-2* is governed by SIR-2.1. We observed that an increased healthy life span due to calorie restriction elicits strong neuroprotective effects. Having observed that RNAi of *nhx-2* is mimicking calorie restriction, we tried to find out the exact molecular mechanism involved in neuroprotection. In one of our previous studies, we have found that calorie restriction and neuroprotection are linked together via SIR-2.1.

Silent information regulator 2 (*Sir-2.1*) proteins, or sirtuins, are protein deacetylases that are found in various organisms, from bacteria to humans. In our previous work calorie restriction was found to show its protective effect only in the presence of *sir-2.1* (17). Keeping that in mind we hypothesized that RNAi of *nhx-2* must be showing its effects via *sir-2.1*. To test this, we have investigated the interplay between *nhx-2* and *sir-2.1* using a combination of RNAi, real-time PCR studies, western blot, pathway mapping via bioinformatics tool GENEMANIA and genetic crossing **.** First of all, we checked whether there is any alteration in the *sir-2.1* levels in the knockdown condition of *nhx-2*. To answer this query, we performed real-time PCR analysis to quantify the levels of *sir-2.1* in *nhx-2* RNAi condition and we found that in the case of *nhx-2* RNAi the level of *sir-2.1* was upregulated significantly. In order to check whether this transcriptional elevation gives rise to increased protein levels of SIR-2.1 we performed a genetic cross between two transgenic strains UL2992 [sir-2.1::mCherry + rol-6(su1006)] that expresses mCherry tagged SIR-2.1 ubiquitously and transgenic strain NL5901 that expresses α-Synuclein intact with its muscles. With the help of a genetic crossing followed by the back cross, we have constructed a strain that expresses mCherry SIR-2.1 ubiquitously and possesses YFP α-Synuclein expression in the muscles. We further performed *nhx-2* RNAi in this strain and we observed that knockdown of *nhx-2* in these worms decreases α-Synuclein expression and increases SIR-2.1 expression. This experiment hence further substantiated our previous finding that *nhx-2* RNAi exerts its neuroprotective effect via increasing the expression of SIR-2.1. It was clear from our previous experiments that *sir-2.1* mRNA levels are up-regulated in *nhx-2* knockdown condition but whether RNAi/knockout of *nhx-2* is affecting the function of SIR-2.1

was yet not clear. To investigate this we procured knock out strain of *nhx-2* and we performed fecundity assay in RNAi background of *sir-2.1* and we found that reproductive helth extension induced by RNAi of *nhx-2* is SIR-2.1 driven.

To decipher the specific mechanistic pathway, we performed pathway analysis with the help of real-time PCR analysis and checked the mRNA levels of various genes critical for several cellular regulatory processes. We found out that amongst all, the genes of mitochondria for example : *atp-2*, *cco-2*, and *gas-2* were significantly modulated. It is also known that calorie restriction via SIRT-2.1 alters mitochondrial biogenesis with increased respiration and enhanced ATP production (41). *nhx-2*, being a proton pump and altering the levels of *sir-2.1* might affect overall mitochondrial health. Hypothesizing that we checked various parameters of mitochondrial health in *C. elegans* including the amount of ATP, number of mitochondria with the help of mitotracker and we have for the first time in *C. elegans* checked the mitochondrial membrane potential of individual cells of *C.elegans* in the knockdown condition of *nhx-2*. We found out that knockdown of *nhx-2* not only elevated the number of mitochondria consequently levels of ATP but also it restored the depolarization of mitochondrial membrane potential in transgenic strain NL5901.

Our observations led us to the conclusion that estradiol connects neuronal health with gut homeostasis via regulating nhx-2 levels which plays a crucial part in food absorption. RNAi of sodium proton pump that is expressed in the intestine *of C. elegans* delayed reproductive senescence and works as a neuroprotectant via decreasing the aggregation of toxic alpha-Synuclein aggregation. Silencing of *nhx-2* elicits a very crucial role in maintaining optimum pH in the gut and facilitates food absorption and also helps in maintaining the food homeostasis. Hence RNAi of *nhx-2* alters the food absorption thereby mimicking CR and increased levels of SIR-2.1 thereafter improving mitochondrial health. We also found that Human estradiol alters the occupancy of epigenetic markers H3K4me3 and H3K9 ac on the promoter region of *nhx-2* thereby altering its expression hence we anticipate that it corroborates in food absorption via increasing *nhx-2* levels. However, we found that this increase did not alter the aggregation of alpha-Synuclein. We hope to further explore the role of Na+/H+ exchangers as sanative for neurodegeneration, further by using this study we can emphasize studying gut health and estradiol induced changes that regulates neuronal health connecting gut to the brain.

1.5 Acknowledgments

Authors thank Prof. Tapas K. Kundu and Dr Sweta Sikder for their valuable comments particularly towards the ChIP assay and in editing the manuscript. Strains used in the study were provided by C. elegans Genetics Center, University of Minnesotta. SS, LK and AS thank UGC/CSIR for their fellowships. AN acknowledges CSIR for funding support. CDRI Communication number : XXXX

1.6 Author Contribution

SS conducted the experiments, analysed data, wrote the manuscript, LK , SK and AS contributed in conducting some of the experiments and towards analyzing data; AN conceived the study, provided infrastructure and reagents, analysed the data and edited the manuscript.

1.7 Conflict of Interest

There is no conflict of interest.

1.8 Data Availability Statement

The data that support the findings of this study are available from the corresponding author upon reasonable request.

References

1. Jafari, S., Etminan, M., Aminzadeh, F., and Samii, A. (2013) Head injury and risk of Parkinson disease: a systematic review and meta-analysis. *Movement disorders : official journal of the Movement Disorder Society* **28**, 1222-1229
2. Meyer, J. S., Rauch, G. M., Rauch, R. A., Haque, A., and Crawford, K. (2000) Cardiovascular and other risk factors for Alzheimer's disease and vascular dementia. *Annals of the New York Academy of Sciences* **903**, 411-423
3. Riess, O., and Kruger, R. (1999) Parkinson's disease--a multifactorial neurodegenerative disorder. *Journal of neural transmission. Supplementum* **56**, 113-125
4. Gunes, S., Hekim, G. N., Arslan, M. A., and Asci, R. (2016) Effects of aging on the male reproductive system. *Journal of assisted reproduction and genetics* **33**, 441-454
5. Hirohata, M., Ono, K., Morinaga, A., Ikeda, T., and Yamada, M. (2009) Anti-aggregation and fibril-destabilizing effects of sex hormones on alpha-synuclein fibrils in vitro. *Experimental neurology* **217**, 434-439

6. Sorvik, I. B., and Paulsen, R. E. (2017) High and low concentration of 17alpha-estradiol protect cerebellar granule neurons in different time windows. *Biochemical and biophysical research communications* **490**, 676-681
7. Woolley, C. S. (2007) Acute effects of estrogen on neuronal physiology. *Annual review of pharmacology and toxicology* **47**, 657-680
8. Zuo, H. L., Deng, Y., Wang, Y. F., Gao, L. L., Xue, W., Zhu, S. Y., Ma, X., and Sun, A. J. (2018) [Effect of low-dose or standard-dose conjugated equine estrogen combined with different progesterone on bone density in menopause syndrome women]. *Zhonghua fu chan ke za zhi* **53**, 243-247
9. Baker, F. C., de Zambotti, M., Colrain, I. M., and Bei, B. (2018) Sleep problems during the menopausal transition: prevalence, impact, and management challenges. *Nature and science of sleep* **10**, 73-95
10. Dalal, P. K., and Agarwal, M. (2015) Postmenopausal syndrome. *Indian journal of psychiatry* **57**, S222-232
11. Sagsoz, N., Oguzturk, O., Bayram, M., and Kamaci, M. (2001) Anxiety and depression before and after the menopause. *Archives of gynecology and obstetrics* **264**, 199-202
12. Drake, E. B., Henderson, V. W., Stanczyk, F. Z., McCleary, C. A., Brown, W. S., Smith, C. A., Rizzo, A. A., Murdock, G. A., and Buckwalter, J. G. (2000) Associations between circulating sex steroid hormones and cognition in normal elderly women. *Neurology* **54**, 599-603
13. Gibbs, R. B., Hashash, A., and Johnson, D. A. (1997) Effects of estrogen on potassium-stimulated acetylcholine release in the hippocampus and overlying cortex of adult rats. *Brain research* **749**, 143-146
14. Singh, A., Asif, N., Singh, P. N., and Hossain, M. M. (2016) Motor Nerve Conduction Velocity In Postmenopausal Women with Peripheral Neuropathy. *Journal of clinical and diagnostic research : JCDR* **10**, CC13-CC16
15. McDonald, R. B., and Ramsey, J. J. (2010) Honoring Clive McCay and 75 years of calorie restriction research. *The Journal of nutrition* **140**, 1205-1210
16. Mattison, J. A., Colman, R. J., Beasley, T. M., Allison, D. B., Kemnitz, J. W., Roth, G. S., Ingram, D. K., Weindruch, R., de Cabo, R., and Anderson, R. M. (2017) Caloric restriction improves health and survival of rhesus monkeys. *Nature communications* **8**, 14063
17. Jadiya, P., Chatterjee, M., Sammi, S. R., Kaur, S., Palit, G., and Nazir, A. (2011) Sir-2.1 modulates 'calorie-restriction-mediated' prevention of neurodegeneration in Caenorhabditis elegans: implications for Parkinson's disease. *Biochemical and biophysical research communications* **413**, 306-310
18. Brenner, S. (1974) The genetics of Caenorhabditis elegans. *Genetics* **77**, 71-94
19. Stiernagle, T. (2006) Maintenance of C. elegans. *WormBook : the online review of C. elegans biology*, 1-11
20. Fraser, A. G., Kamath, R. S., Zipperlen, P., Martinez-Campos, M., Sohrmann, M., and Ahringer, J. (2000) Functional genomic analysis of C. elegans chromosome I by systematic RNA interference. *Nature* **408**, 325-330
21. Ahmed, F., Kumar, M., and Raghava, G. P. (2009) Prediction of polyadenylation signals in human DNA sequences using nucleotide frequencies. *In silico biology* **9**, 135-148
22. Gurusaran, M., Ravella, D., and Sekar, K. (2013) RepEx: repeat extractor for biological sequences. *Genomics* **102**, 403-408

23. van Dijk, M., and Bonvin, A. M. (2009) 3D-DART: a DNA structure modelling server. *Nucleic acids research* **37**, W235-239
24. Kim, S., Chen, J., Cheng, T., Gindulyte, A., He, J., He, S., Li, Q., Shoemaker, B. A., Thiessen, P. A., Yu, B., Zaslavsky, L., Zhang, J., and Bolton, E. E. (2019) PubChem 2019 update: improved access to chemical data. *Nucleic acids research* **47**, D1102-D1109
25. UniProt, C. (2019) UniProt: a worldwide hub of protein knowledge. *Nucleic acids research* **47**, D506-D515
26. Jendele, L., Krivak, R., Skoda, P., Novotny, M., and Hoksza, D. (2019) PrankWeb: a web server for ligand binding site prediction and visualization. *Nucleic acids research* **47**, W345-W349
27. Morris, G. M., Huey, R., and Olson, A. J. (2008) Using AutoDock for ligand-receptor docking. *Current protocols in bioinformatics* **Chapter 8**, Unit 8 14
28. Macindoe, G., Mavridis, L., Venkatraman, V., Devignes, M. D., and Ritchie, D. W. (2010) HexServer: an FFT-based protein docking server powered by graphics processors. *Nucleic acids research* **38**, W445-449
29. Tian, W., Chen, C., Lei, X., Zhao, J., and Liang, J. (2018) CASTp 3.0: computed atlas of surface topography of proteins. *Nucleic acids research* **46**, W363-W367
30. Mahmood, T., and Yang, P. C. (2012) Western blot: technique, theory, and trouble shooting. *North American journal of medical sciences* **4**, 429-434
31. Sikder, S., Kumari, S., Mustafi, P., Ramdas, N., Padhi, S., Saha, A., Bhaduri, U., Banerjee, B., Manjithaya, R., and Kundu, T. K. (2019) Nonhistone human chromatin protein PC4 is critical for genomic integrity and negatively regulates autophagy. *The FEBS journal* **286**, 4422-4442
32. Wang, M. C., Oakley, H. D., Carr, C. E., Sowa, J. N., and Ruvkun, G. (2014) Gene pathways that delay Caenorhabditis elegans reproductive senescence. *PLoS genetics* **10**, e1004752
33. Uttara, B., Singh, A. V., Zamboni, P., and Mahajan, R. T. (2009) Oxidative stress and neurodegenerative diseases: a review of upstream and downstream antioxidant therapeutic options. *Current neuropharmacology* **7**, 65-74
34. King, L. A., Priest, K. C., Nutt, J., Chen, Y., Chen, Z., Melnick, M., and Horak, F. (2014) Comorbidity and functional mobility in persons with Parkinson disease. *Archives of physical medicine and rehabilitation* **95**, 2152-2157
35. Brinton, R. D., Tran, J., Proffitt, P., and Montoya, M. (1997) 17 beta-Estradiol enhances the outgrowth and survival of neocortical neurons in culture. *Neurochemical research* **22**, 1339-1351
36. Whittle, J. R., Powell, M. J., Popov, V. M., Shirley, L. A., Wang, C., and Pestell, R. G. (2007) Sirtuins, nuclear hormone receptor acetylation and transcriptional regulation. *Trends in endocrinology and metabolism: TEM* **18**, 356-364
37. Stark, C., Breitkreutz, B. J., Reguly, T., Boucher, L., Breitkreutz, A., and Tyers, M. (2006) BioGRID: a general repository for interaction datasets. *Nucleic acids research* **34**, D535-539
38. Nehrke, K. (2003) A reduction in intestinal cell pHi due to loss of the Caenorhabditis elegans Na+/H+ exchanger NHX-2 increases life span. *The Journal of biological chemistry* **278**, 44657-44666

39. Arnold, S. (2012) Cytochrome c oxidase and its role in neurodegeneration and neuroprotection. *Advances in experimental medicine and biology* **748**, 305-339
40. Brinton, R. D., Chen, S., Montoya, M., Hsieh, D., and Minaya, J. (2000) The estrogen replacement therapy of the Women's Health Initiative promotes the cellular mechanisms of memory and neuronal survival in neurons vulnerable to Alzheimer's disease. *Maturitas* **34 Suppl 2**, S35-52
41. Nisoli, E., Tonello, C., Cardile, A., Cozzi, V., Bracale, R., Tedesco, L., Falcone, S., Valerio, A., Cantoni, O., Clementi, E., Moncada, S., and Carruba, M. O. (2005) Calorie restriction promotes mitochondrial biogenesis by inducing the expression of eNOS. *Science* **310**, 314-317

Legends

Figure 1:

Systematic preliminary screening of genes that delay reproductive senescence in *C. elegans* in regard to various endpoints of neurodegeneration .(a) RNAi of 22 genes available and their effect on α-Syn accumulation: The aggregation of α-Syn was assayed in NL5901 [unc54p::alpha-Synuclein:: YFP+unc-119(+)], a transgenic strain of C. elegans that expresses human α-Syn:: YFP transgene in their body wall muscles. All images used the same exposure time and gain settings; Scale bar=100µm. (b) Graphical representation for α-Syn aggregation in transgenic strain NL5901.(c) Effect of RNAi silencing of the various candidates on the relative formation of reactive oxygen (ROS) measured by H2DCFDA assay. H2DCFDA is a chemically reduced, non-fluorescent acetylated form of fluorescein which is readily converted to a green fluorescent form by the activity of ROS. An imbalance between the formation and transmission of ROS has been co-related with PD pathogenesis and can exacerbate its progression. d) Effect of RNAi silencing of the 22 genes on the number of thrashes in transgenic strain NL5901 of *C. elegans*. The intensity of fluorescence was measured using ImageJ software and Significance was determined using Student's t-test *p<0.05,**p<0.01,***p<0.001,ns-non-significant.

Figure 2:

Western blot and immunoblot analysis of α-Synuclein protein using anti aggregated α-Synuclein antibody: (a-b): Represents the immunoblot analysis of aggregated α-Synuclein protein.Bands in first row represent aggregated α-Synuclein expression upon silencing of screened genes namely EV, *nhx-2, F20B10.2, F25H8.1, T04B2.1, VC27A7L.1, ilys-3, rskn-1* respectively ,whereas bands in the second row represent control Actin, a housekeeping protein. Significance was determined using a Student's t-test *p<0.05,**p<0.01,***p<0.001,ns-non-significant. (c-d) : 17-β-estradiol treatment in C. elegans altered the transcripts of *nhx-2*. qPCR analysis of estradiol responding genes vit-2 and vit-6 at different concentrations in wild type strain *p<0.05,ns-non significant. Real-time PCR analysis of screened genes after estradiol treatment over untreated control group in transgenic strain NL5901; Revealed estradiol treatment modulates *nhx-2* levels.Significance was determined using a Student's t-test *p<0.05,**p<0.01,***p<0.001,ns-non-significant. (e-f): Interaction between Nuclear Hormonal Receptor and *nhx-2*, A) Docking of NHR-14 receptor-estradiol complex with *nhx-2* inverse repeat contig(AGTTGCAATACTA,1431-1443,5'-3'). (B) There is an active interaction between the NHR-14 complex and DNA contig in DNA binding site. Participating residues are PHE,ARG,TRP,GLN,ASN,VAL,LEU,LYS,SER

Figure 3:

ChIP analysis demonstrating estradiol treatment increases the occupancy of H3K9ac and H3K4me3 activation marker on the promoter region of *nhx-2*. (a) qPCR analysis demonstrating significant upregulation of *nhx-2* upon estradiol treatment, data is presented as ± SEM (n=2), Significance **p<0.01 (b) This image shows the effect of estradiol treatment on H3K9 acetylation at the global genomic level. While the global expression of H3K9ac was found to be significantly increased we found no significant alteration of H3K4me3. The significance level was determined using ImageJ analysis followed by graph pad where significance levels were calculated as **p<0.01, ns-non-significant (c) The image represents different sizes of DNA fragments (200bp) after sonication with the help of agarose gel electrophoresis. (d-e) Occupancy of H3K9ac and H3K4me3 activation markers at the promoter region of the *nhx-2* gene were evaluated with the help of ChIP analysis, using the H3K9Ac and H3K4me3 antibodies in both

untreated and estradiol treated groups followed by qPCR analysis using specific primers of the promoter regions. Data are presented as ± SEM (n=2), Significance **p<0.01,ns-non-significant.

Figure 4:

Estradiol treatment increases *nhx-2* expression although it doesn't give rise to increased α-Syn aggregated protein and RNAi/Knockout of *nhx-2* alters food absorption, accelerates sir-2.1 expression and functionality. (a)This figure represents results of the immunoblot experiment in which bands of the first row represent α-Syn aggregated protein in control, *nhx-2*-RNAi and worms treated with estradiol respectively whereas bands in the second row represent housekeeping protein GAPDH. Significance was determined using a Student's t-test *p<0.05, ns-non-significant. (b) This image panel represents fluorescent OP50 in the gut of NL5901 and Knockout strain of *nhx-2*: VC363.A-B in the panel represents anterior and posterior parts of the worm NL5901 and C-D in the panel represents anterior and posterior parts of the KO strain of *nhx-2* VC363. Arrows in image C-D points unabsorbed food that remained in the gut, thereafter the entire gut is showing fluorescence. (c) This figure represents qPCR analysis of mRNA levels of *sir-2.1* upon *nhx-2* RNAi. Significance was determined using a Student's t-test **p<0.001. (d) RNAi of *nhx-2* increased the reproductive life span by five days in transgenic strain NL5901 but this alteration of the reproductive life span was not shown in the RNAi condition of sir-2.1.

Figure 5:

Creation of transgenic strains that express SIR-2.1 all over the body and alpha-synuclein in its muscles revealed that *nhx-2* RNAi decreases α-synuclein via up-regulating the expression of SIR-2.1 .(A-C) Confocal images of the wild type strain in FITC, Rhodamine and brightfield (D-F) Confocal images of crossed EV worms in FITC, Rhodamine and merged image (G-I) Confocal images of crossed worms given *nhx-2* RNAi treatment in FITC, Rhodamine and merged image

Figure 6:

***nhx-2* RNAi improves overall mitochondrial health and restores the mitochondrial membrane depolarization in transgenic strain NL5901**. (a) qPCR analysis of selected genes of various pathways in transgenic model NL5901. The level of gene atp-2 is significantly up-

regulated whereas the level of genes gas-2 and cco-2 is significantly down-regulated.*p<0.05,ns-nonsignificant.b) ATP measurements: The level of ATP was significantly up-regulated in worms with *nhx-2* RNAi treatment. Significance was determined using a Student's t-test (*denotes p< 0.05 as compared to the wild-type,***denotes p<0.001 as compared to the wild type). Data represent mean±SEM. c) The effect of knockdown of *nhx-2* on mitochondrial content in transgenic strain NL5901 of C.elegans that expresses human α-Syn:: YFP transgene in their body wall muscles. All images used the same exposure time and gain setting, Scale bar=20µm.d) RNAi of *nhx-2* restores depolarization of mitochondrial membrane; 1) Mitochondrial membrane potential [MMP] of wild type N2 strain, in wild type N2 strain the j-aggregates are lower which shows that the membrane is depolarised,2) MMP of transgenic worms NL5901 expressing α-Syn. The mitochondrial membrane is polarized which is indicated by higher j aggregates.3) RNAi of *nhx-2* restores the depolarization of mitochondrial potential in transgenic strain NL5901 as evident from the image it decreases j aggregates significantly .e) MMP ratio of red vs green cells to measure the MMP change in wild type, EV, NL5901, and *nhx-2* RNAi conditions. Significance *p<0.05,**p<0.001.

Table 1: Compilation of docking analysis

Table 2:Sequences of primers used in the real-time analysis and other experiments

Supplementary figure :

Figure S-1: Interaction between Nuclear Hormonal Receptor and query gene (A)Docking of NHR-14 receptor -estradiol complex with *nhx-2* inverse repeat contig (GAAAAATTGTTCTA,1644-1677,5'-3').(B) There is no interaction between the NHR-14 and DNA in DNA binding site.

Figure S-2: Interaction between Nuclear Hormonal Receptor and query gene (A)Docking of NHR-14 receptor -estradiol complex with her-1 inverse repeat contig (TTTCATATCT,1578-1587,5'-3').(B) There is an interaction between the NHR-14 complex and DNA contig in DNA binding site. Participating residues are ARG,SER,VAL,TRP,GLN,ASN,LEU,GLU,TYR,THR,PRO,GLY,ILE.

Figure S-3: Schematic representation of food absorption

1.

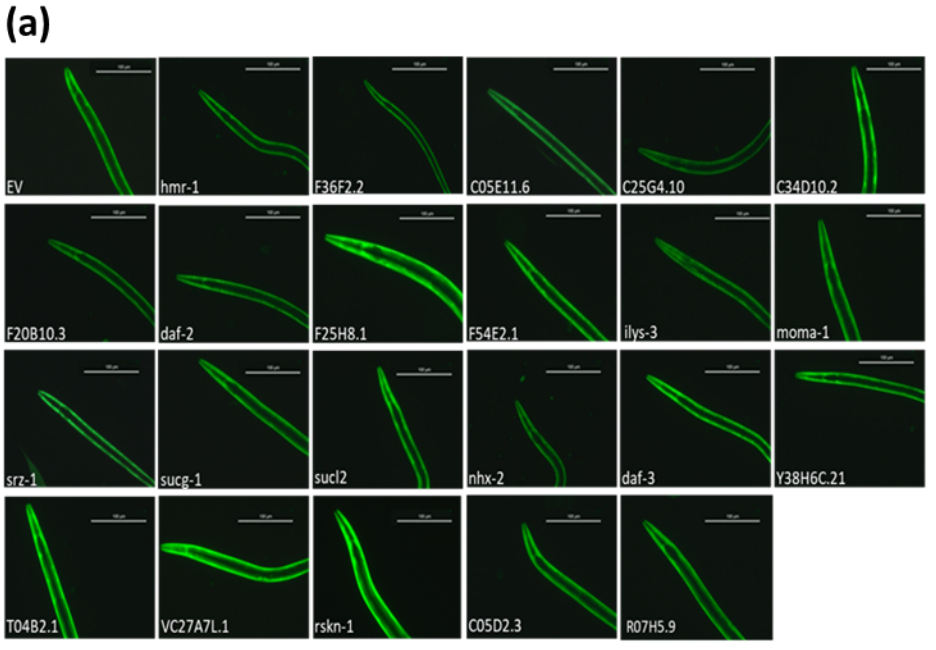
(a)
EV
hmr-1
F36F2.2
C05E11.6
C25G4.10
C34D10.2
F20B10.3
daf-2
F25H8.1
F54E2.1
ilys-3
moma-1
srz-1
sucg-1
sucl2
nhx-2
daf-3
Y38H6C.21
T04B2.1
VC27A7L.1
rskn-1
C05D2.3
R07H5.9

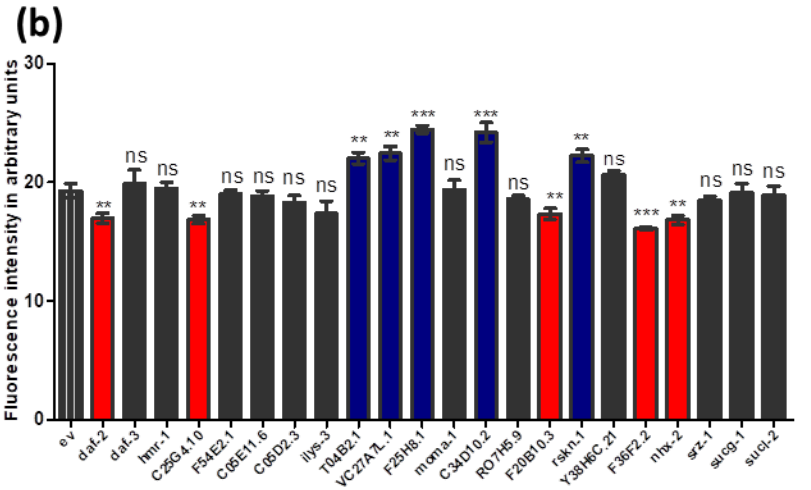
(b)
Fluorescence intensity in arbitrary units
30
20
10
0
ev
daf-2
daf-3
hmr-1
C25G4.10
F54E2.1
C05E11.6
C05D2.3
ilys-3
T04B2.1
VC27A7L.1
F25H8.1
moma-1
C34D10.2
R07H5.9
F20B10.3
rskn-1
Y38H6C.21
F36F2.2
nhx-2
srz-1
sucg-1
sucl-2

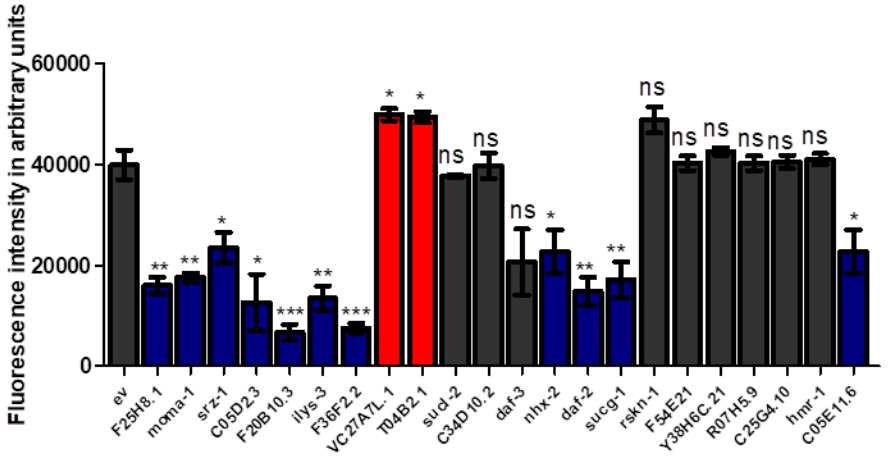
(c)
Fluorescence intensity in arbitrary units
60000
40000
20000
0
ev
F25H8.1
moma-1
srz-1
C05D2.3
F20B10.3
ilys-3
F36F2.2
VC27A7L.1
T04B2.1
sucl-2
C34D10.2
daf-3
nhx-2
daf-2
sucg-1
rskn-1
F54E21
Y38H6C.21
R07H5.9
C25G4.10
hmr-1
C05E11.6

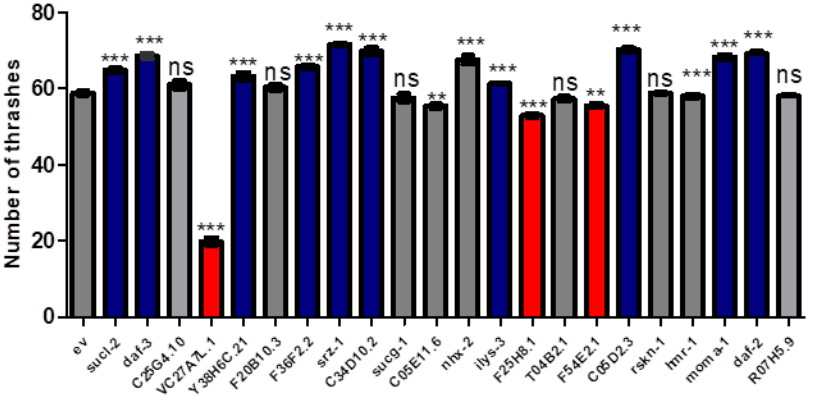
(d)
Number of thrashes
80
60
40
20
0
ev
sucl-2
daf-3
C25G4.10
VC27A7L.1
Y38H6C.21
F20B10.3
F36F2.2
srz-1
C34D10.2
sucg-1
C05E11.6
nhx-2
ilys-3
F25H8.1
T04B2.1
F54E2.1
C05D2.3
rskn-1
hmr-1
moma-1
daf-2
R07H5.9

2.

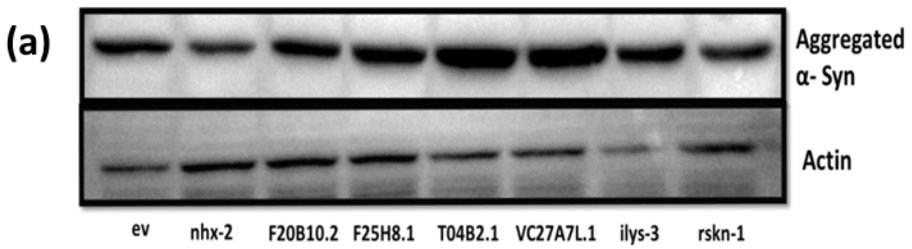
(a)
Aggregated α- Syn
Actin
ev
nhx-2
F20B10.2
F25H8.1
T04B2.1
VC27A7L.1
ilys-3
rskn-1

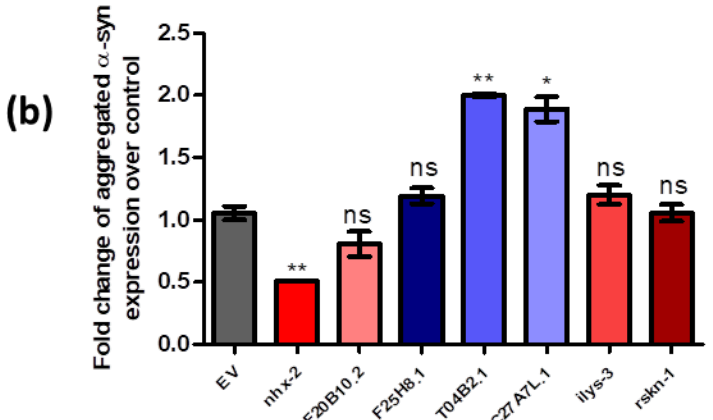
(b)
Fold change of aggregated α-syn expression over control
2.5
2.0
1.5
1.0
0.5
0.0
**
ns
ns
ns
**
*
ns
ns
EV
nhx-2
F20B10.2
F25H8.1
T04B2.1
VC27A7L.1
ilys-3
rskn-1

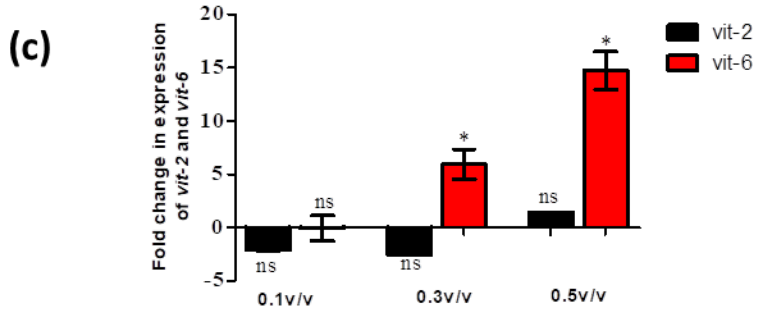
(c)
Fold change in expression of vit-2 and vit-6
20
15
10
5
0
-5
ns
ns
*
ns
*
vit-2
vit-6
0.1v/v
0.3v/v
0.5v/v

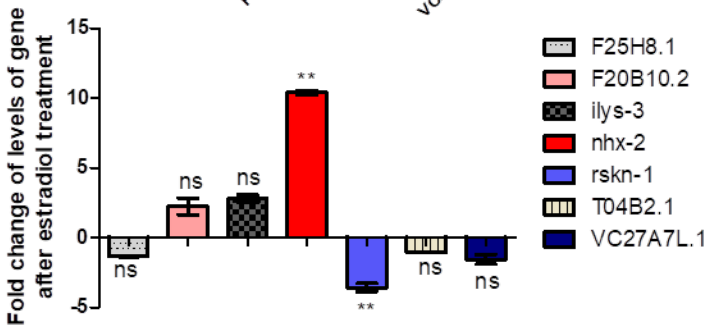
(d)
Fold change of levels of gene after estradiol treatment
15
10
5
0
-5
ns
ns
ns
**
**
ns
ns
F25H8.1
F20B10.2
ilys-3
nhx-2
rskn-1
T04B2.1
VC27A7L.1

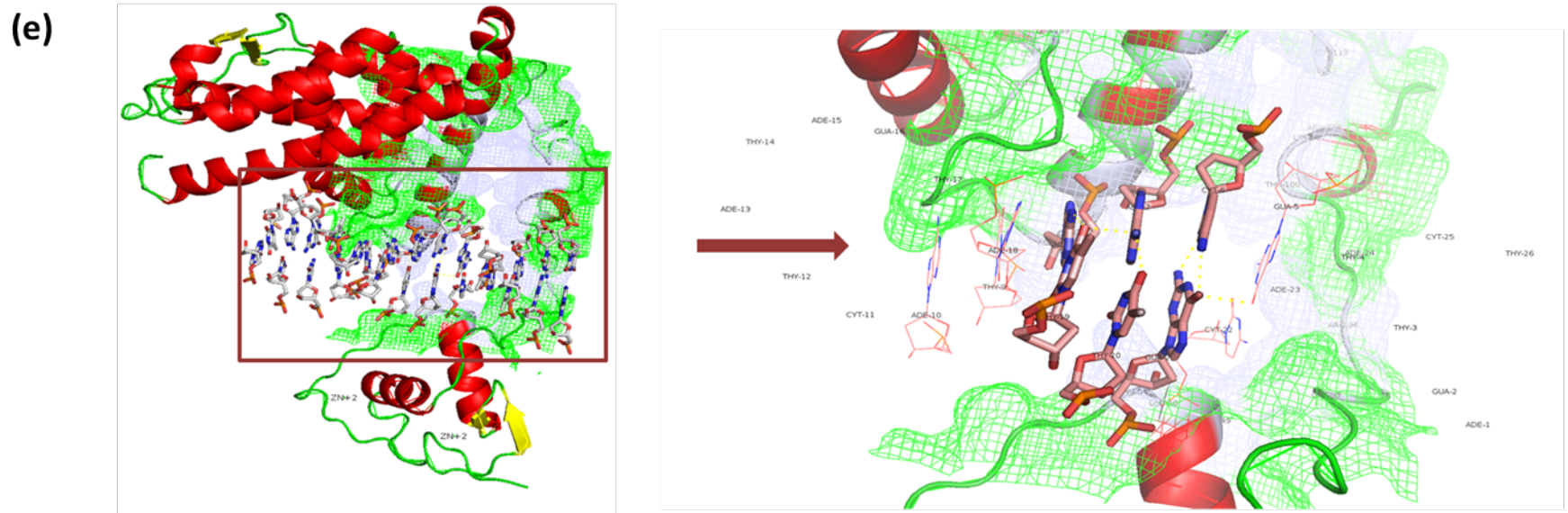
(e)
ZN+2
ZN+2

3. (a)

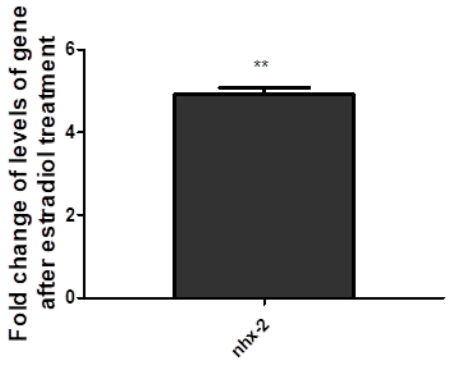
Fold change of levels of gene after estradiol treatment
6
4
2
0
**
nhx-2

(b)

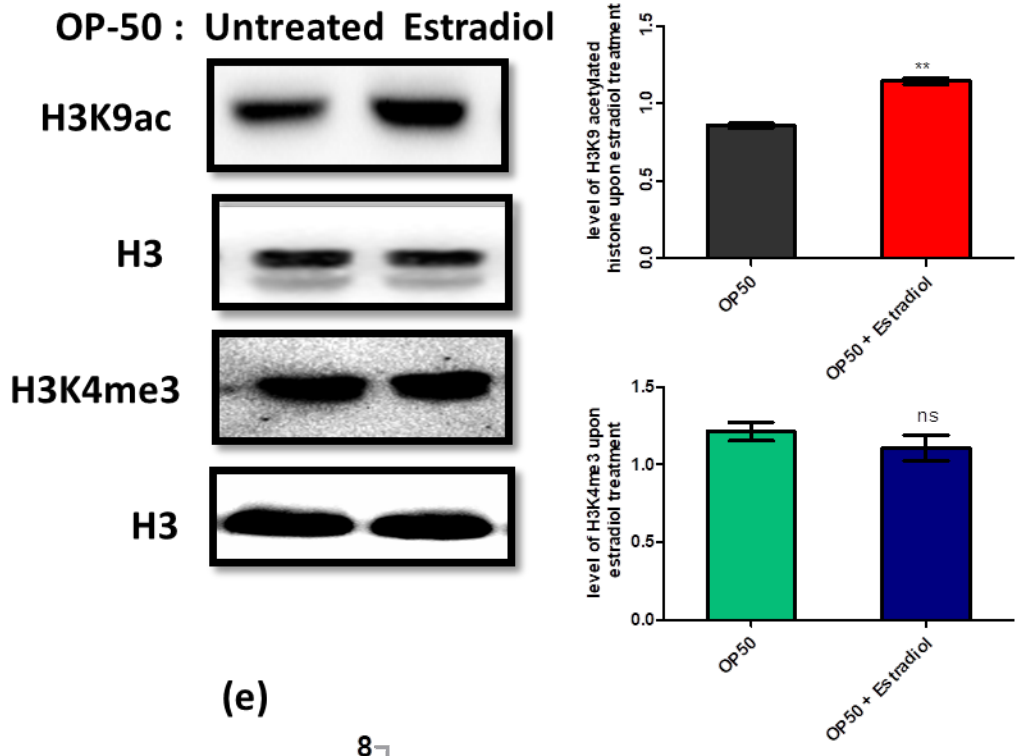
OP-50 : Untreated Estradiol
H3K9ac
H3
H3K4me3
H3
level of H3K9 acetylated histone upon estradiol treatment
1.5
1.0
0.5
0.0
**
OP50
OP50 + Estradiol
level of H3K4me3 upon estradiol treatment
1.5
1.0
0.5
0.0
ns
OP50
OP50 + Estradiol

(c)

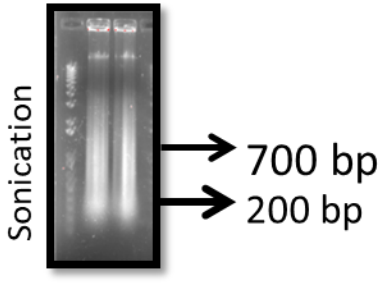
Sonication
700 bp
200 bp

(d)

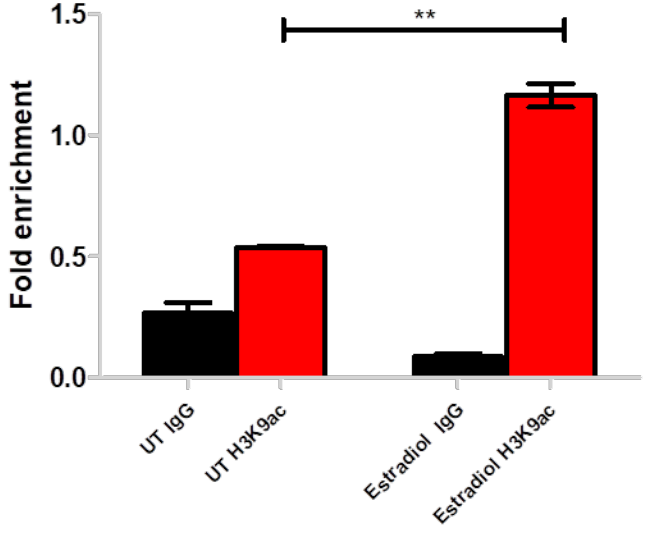
Fold enrichment
1.5
1.0
0.5
0.0
**
UT IgG
UT H3K9ac
Estradiol IgG
Estradiol H3K9ac

(e)

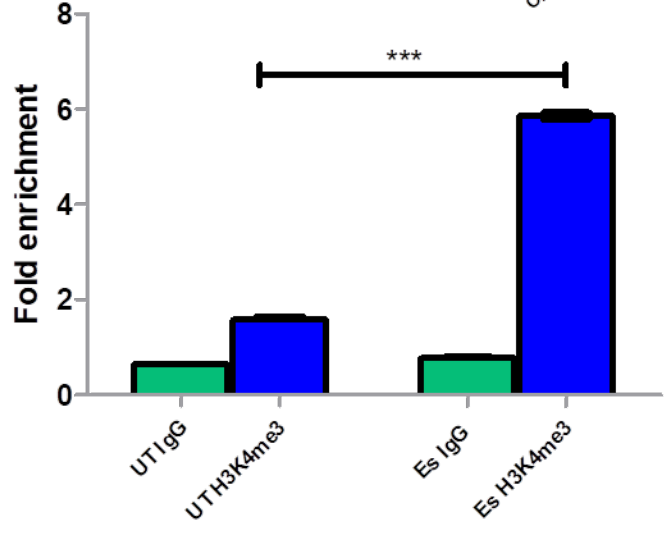
Fold enrichment
8
6
4
2
0
***
UT IgG
UT H3K4me3
Es IgG
Es H3K4me3

Feed:OP50

Feed:OP50 + 17-β-Estradiol

Strain: NL5901

GOI: *nhx-2*
Position: Chr II:7690711..7695324

Promoter-1
chrII:7693950-7694430

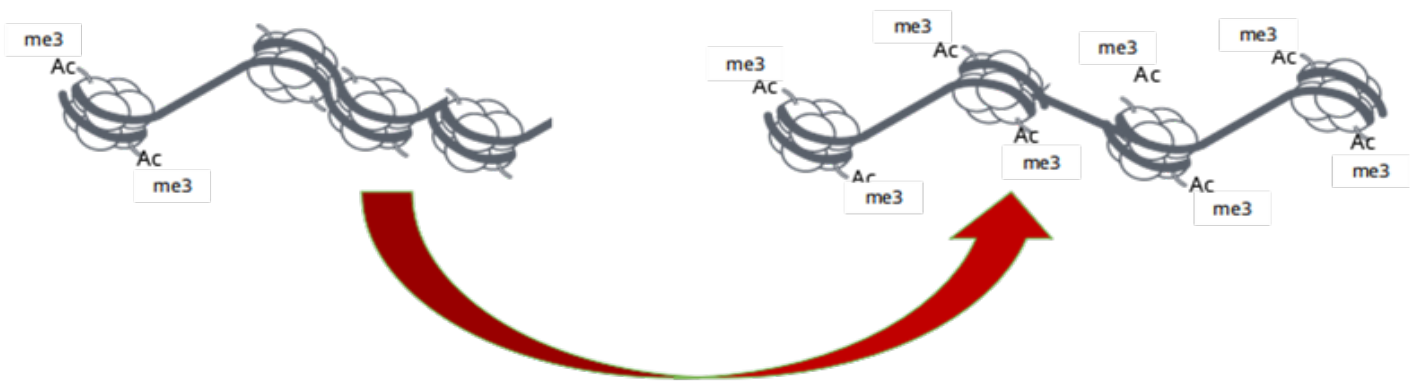

Increase in H3K9 Acetylation and H3K4 Trimethylation activation markers in promoter region of *nhx-2* upon 17-β-Estradiol treatment

4. (a)

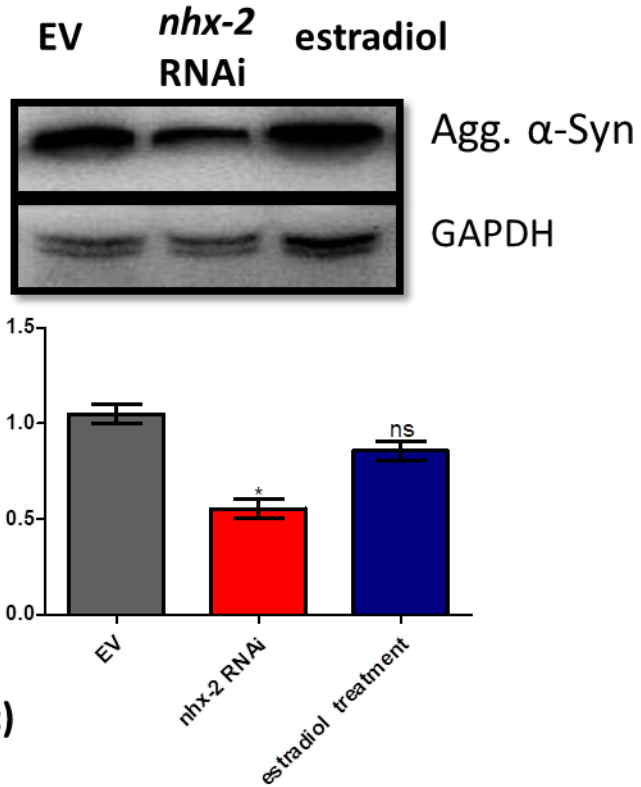
EV
nhx-2 RNAi
estradiol
Agg. α-Syn
GAPDH
Fold change of α-syn aggregation over control
1.5
1.0
0.5
0.0
*
ns
EV
nhx-2 RNAi
estradiol treatment

(b)

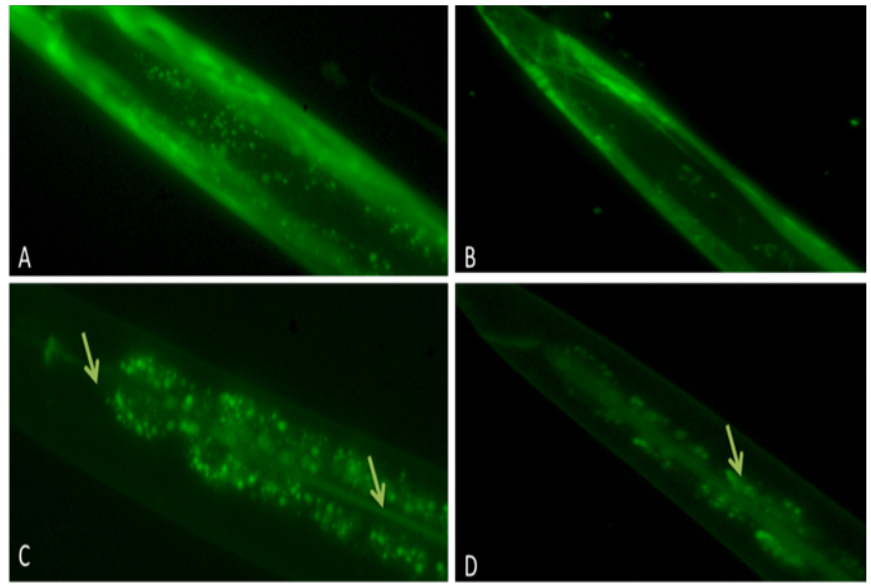
A
B
C
D

(c)

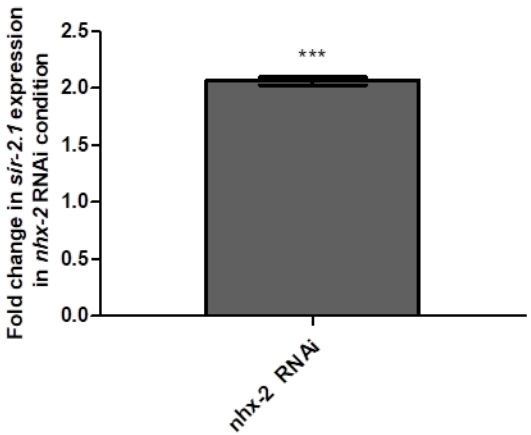
Fold change in sir-2.1 expression in nhx-2 RNAi condition
2.5
2.0
1.5
1.0
0.5
0.0
***
nhx-2 RNAi

(d)

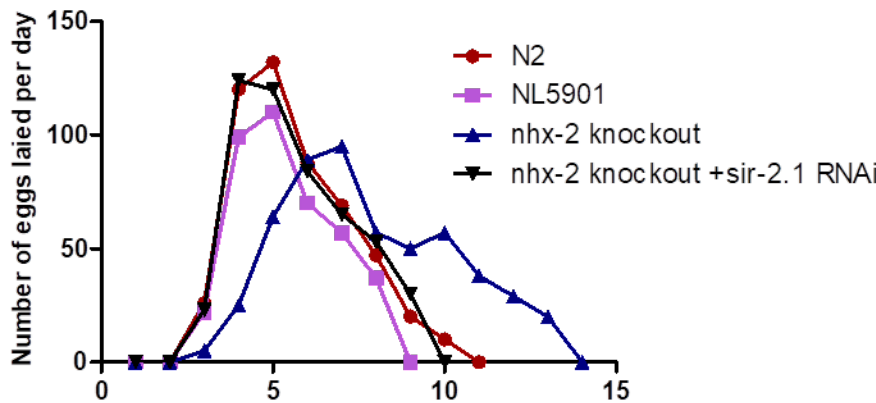
Number of eggs laied per day
150
100
50
0
0
5
10
15
N2
NL5901
nhx-2 knockout
nhx-2 knockout +sir-2.1 RNAi

5.

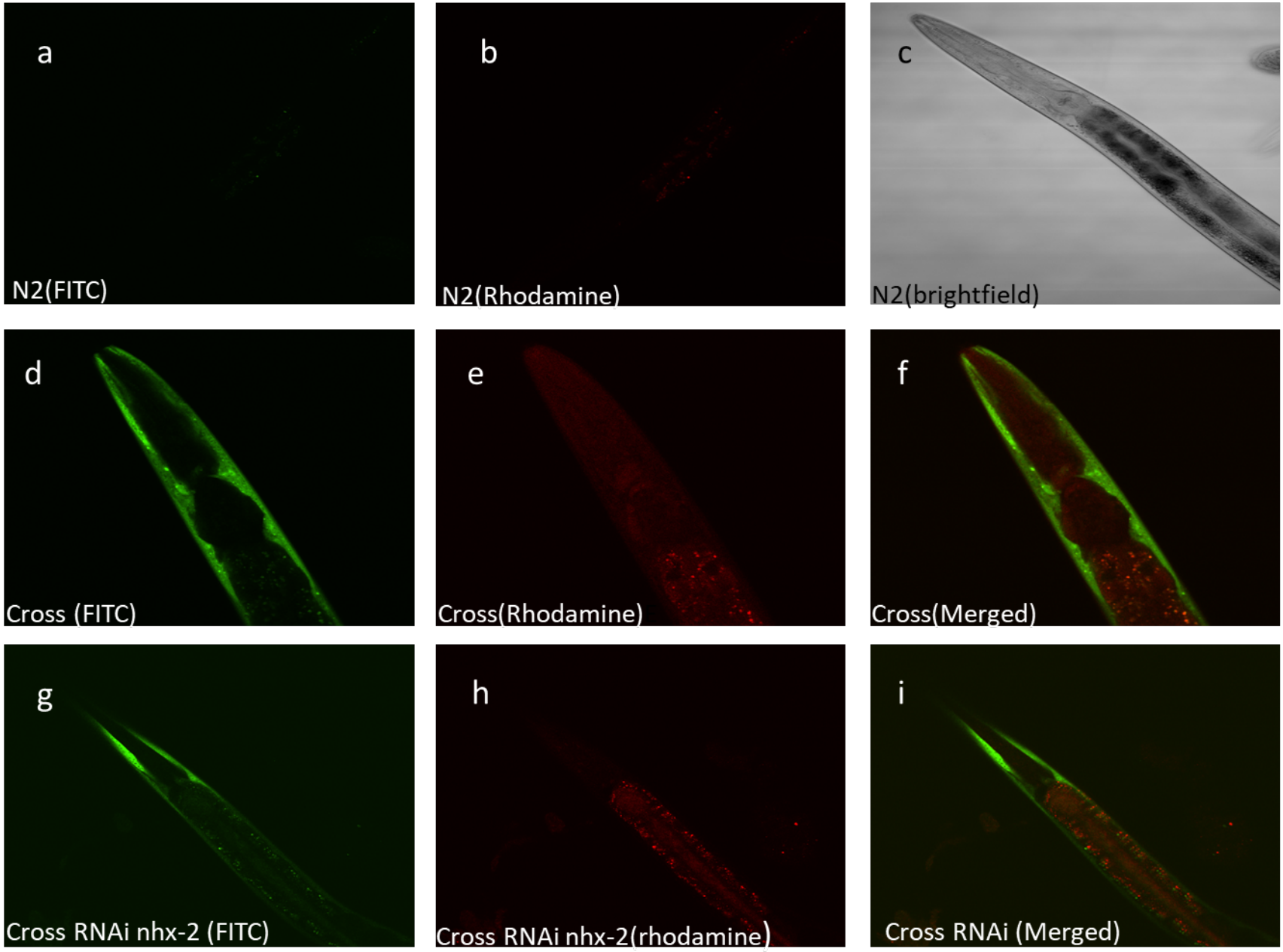
a
N2(FITC)
b
N2(Rhodamine)
c
N2(brightfield)
d
Cross (FITC)
e
Cross(Rhodamine)
f
Cross(Merged)
g
Cross RNAi nhx-2 (FITC)
h
Cross RNAi nhx-2(rhodamine)
i
Cross RNAi (Merged)

6.

(a)

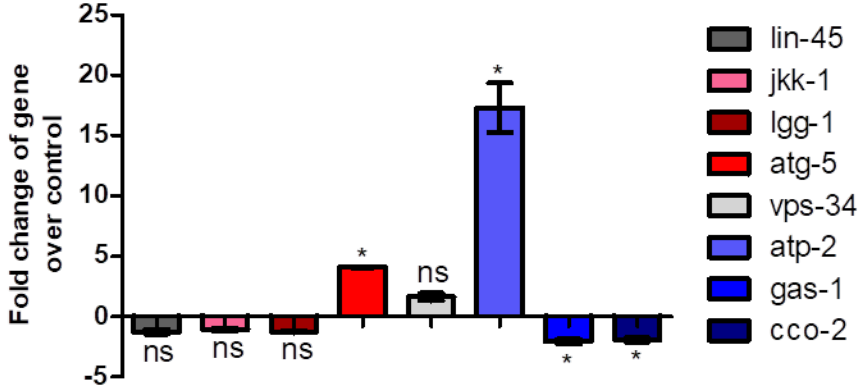
Fold change of gene over control
25
20
15
10
5
0
-5
ns
ns
ns
*
ns
*
*
*
lin-45
jkk-1
lgg-1
atg-5
vps-34
atp-2
gas-1
cco-2

(b)

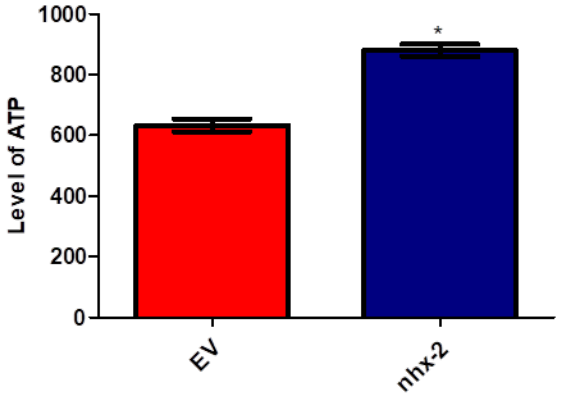
Level of ATP
1000
800
600
400
200
0
*
EV
nhx-2

(c)

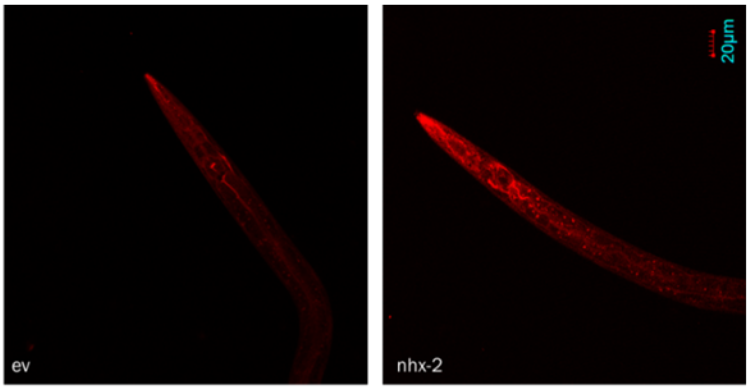
20µm
ev
nhx-2

(d)

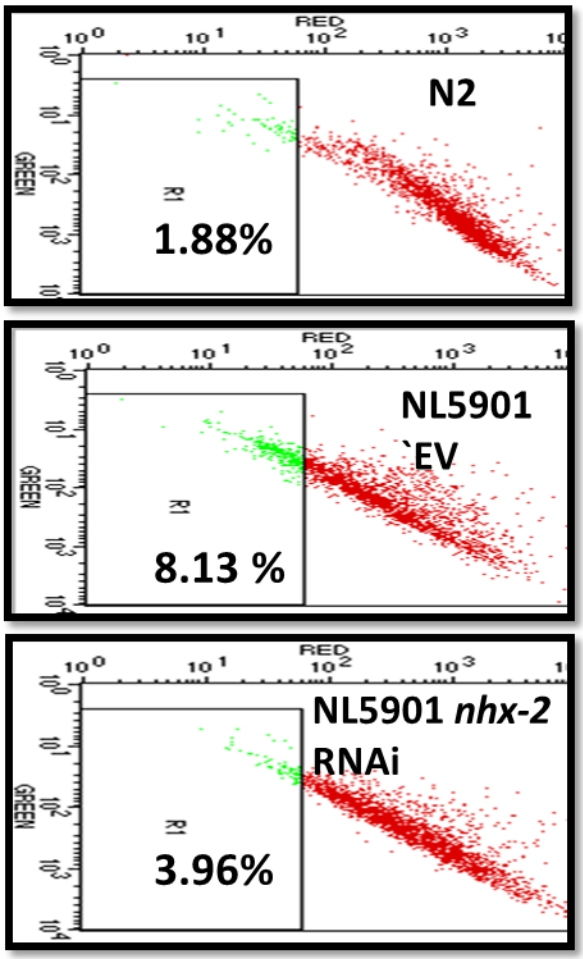
RED
GREEN
N2
R1
1.88%
NL5901
EV
8.13 %
NL5901 nhx-2
RNAi
3.96%

(e)

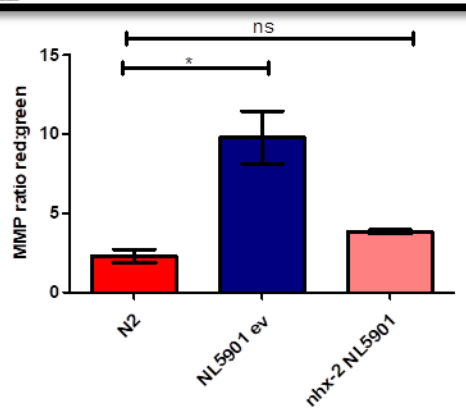
ns
*
MMP ratio red:green
15
10
5
0
N2
NL5901 ev
nhx-2 NL5901

S-2A

S-2B

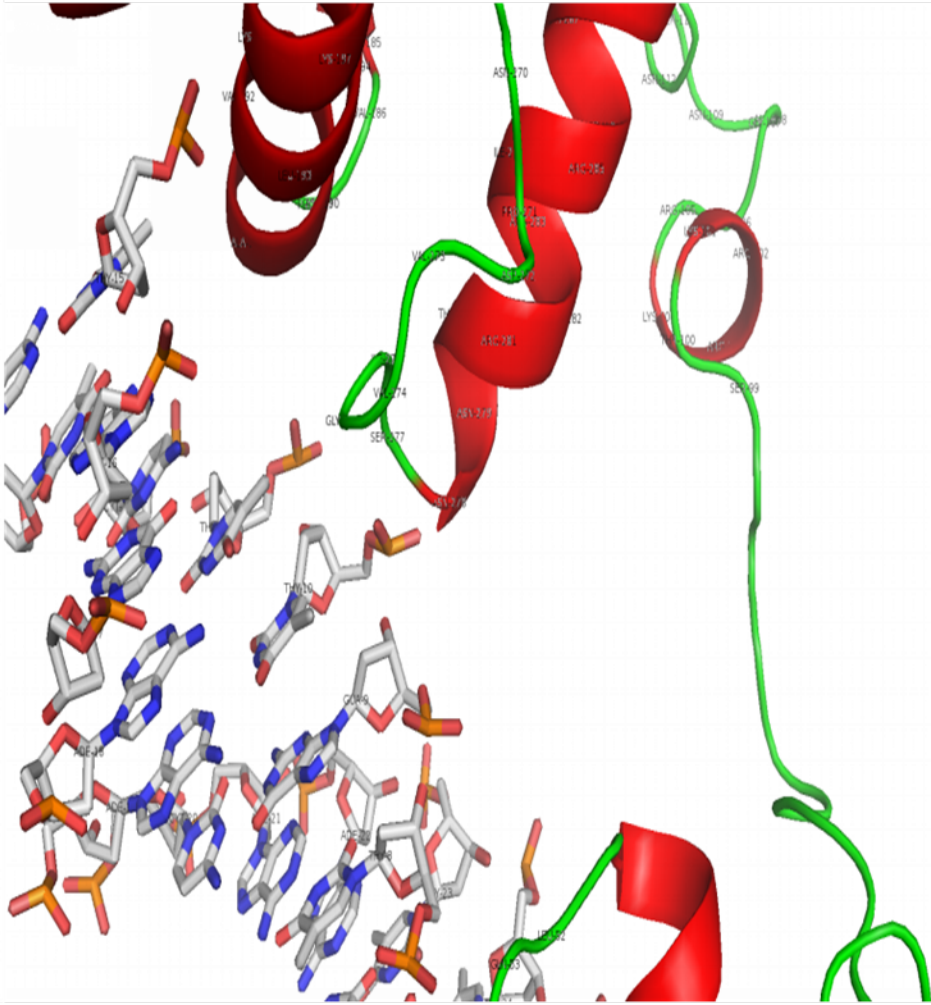

S-3A

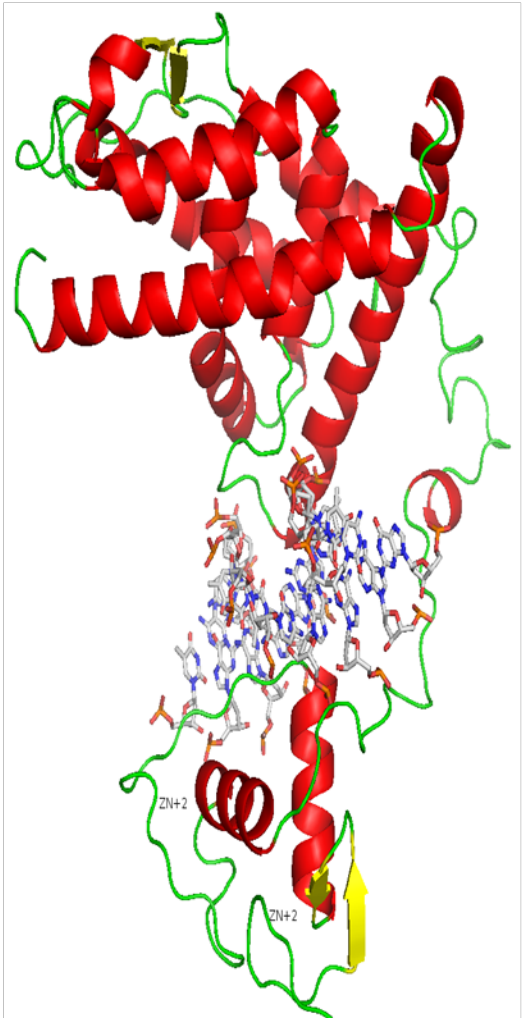
ZN+2
ZN+2

S-3B

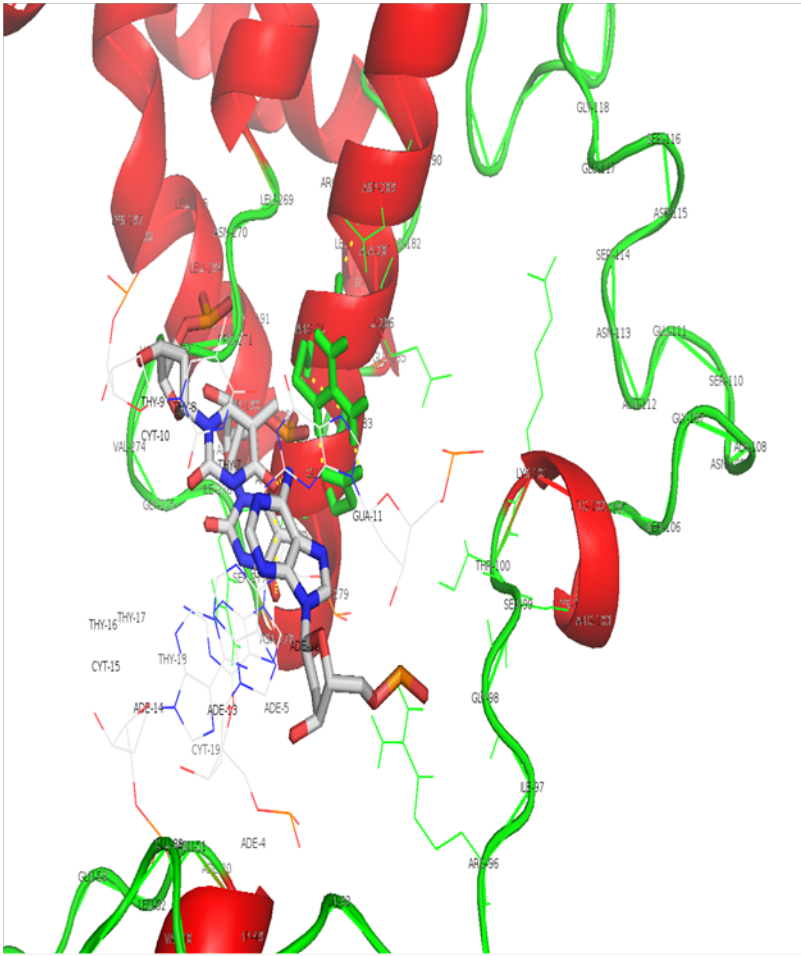
GLY-118
SER-116
ASN-115
SER-114
ASN-113
SER-110
ASN-108
GUA-11
THY-9
CYT-10
VAL-74
THY-16
THY-17
CYT-15
THY-19
ADE-14
ADE-13
ADE-5
CYT-19
ADE-4
GLY-68
ILE-97
ARG-96

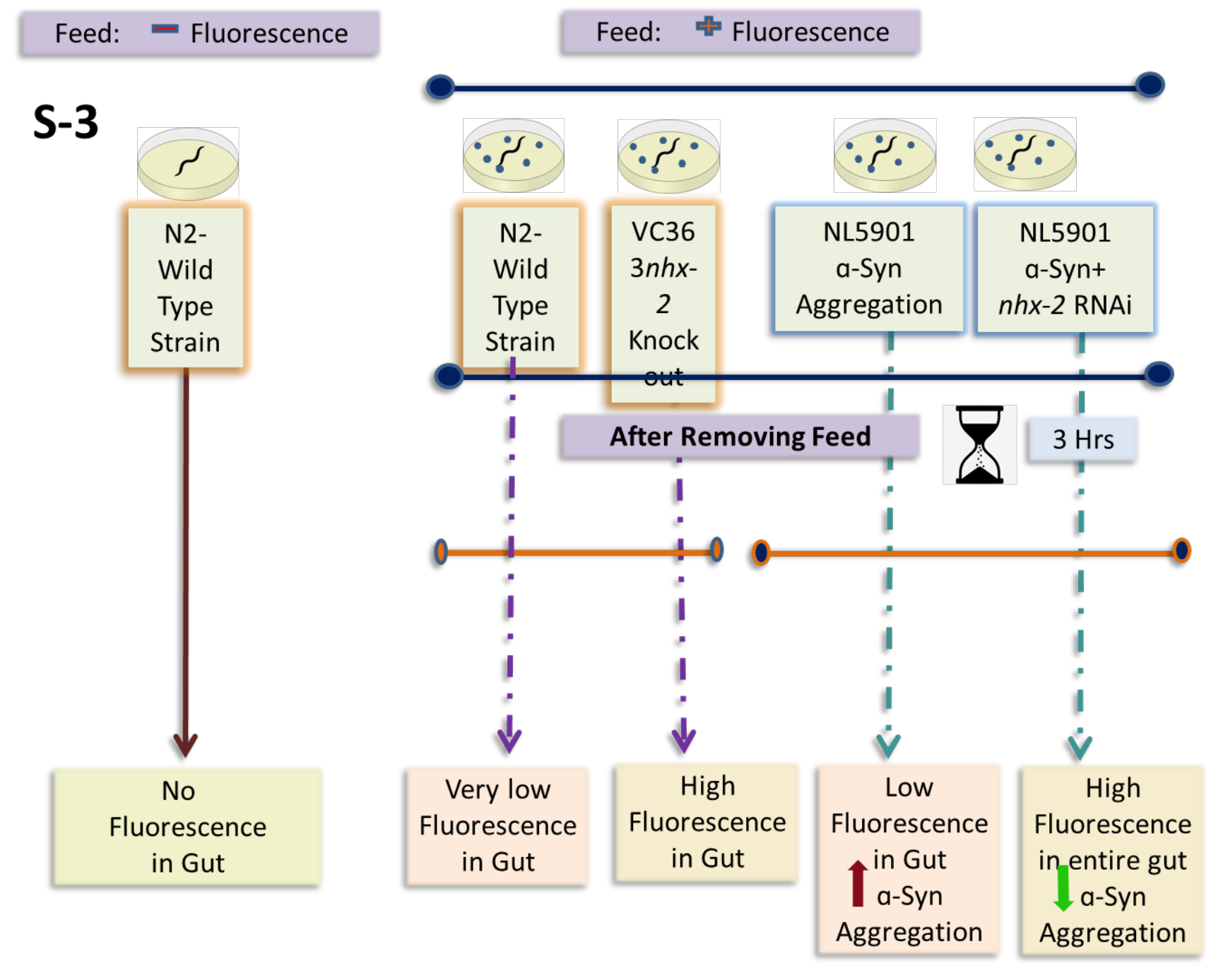
Feed: Fluorescence
Feed: Fluorescence
S-3
N2- Wild Type Strain
N2- Wild Type Strain
VC36 3nhx-2 Knock out
NL5901 α-Syn Aggregation
NL5901 α-Syn+ nhx-2 RNAi
After Removing Feed
3 Hrs
No Fluorescence in Gut
Very low Fluorescence in Gut
High Fluorescence in Gut
Low Fluorescence in Gut α-Syn Aggregation
High Fluorescence in entire gut α-Syn Aggregation